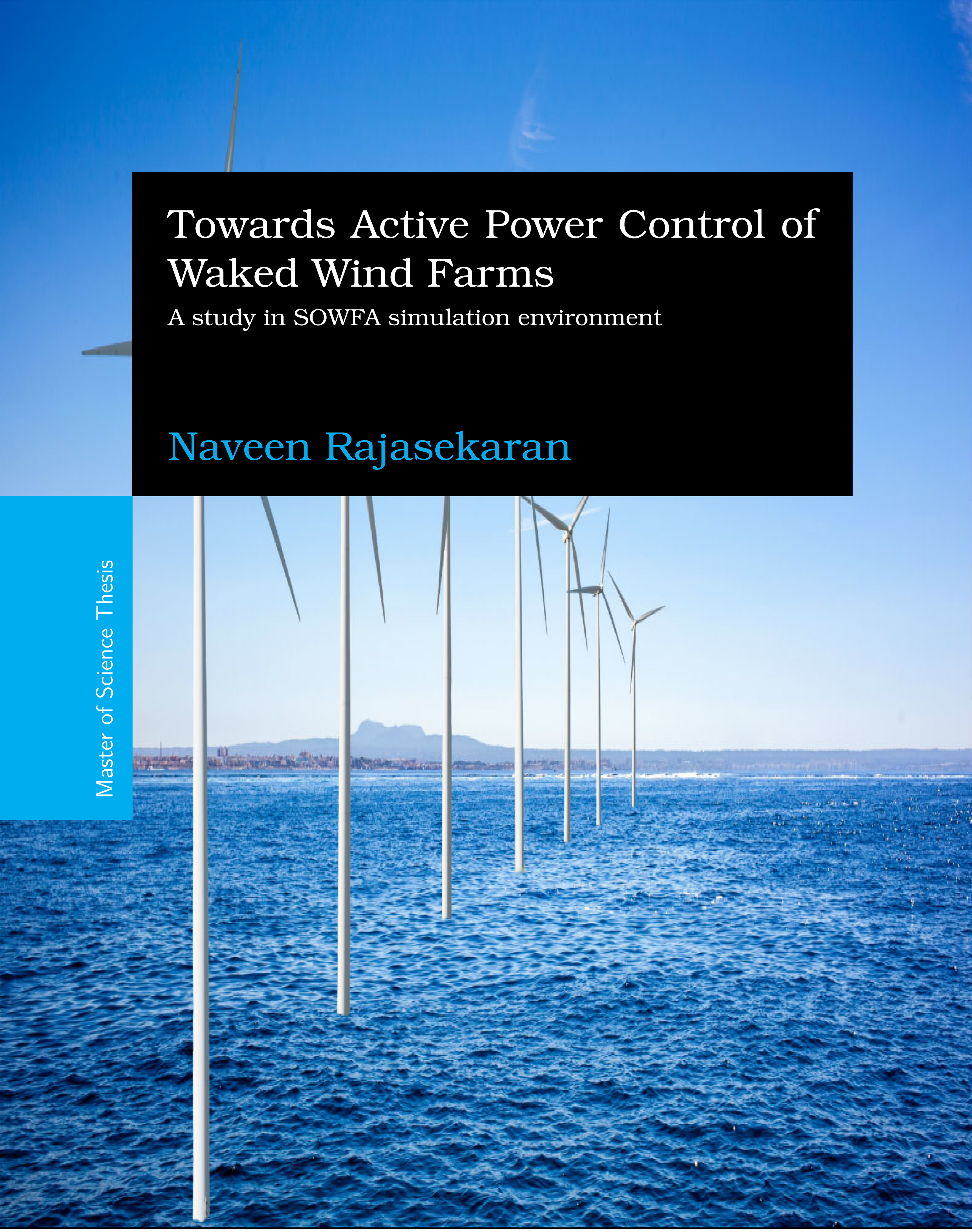

Towards Active Power Control of Waked Wind Farms

A study in SOWFA simulation environment

Naveen Rajasekaran

Master of Science Thesis

Delft University of Technology

Delft Center for Systems and Control

Towards Active Power Control of Waked Wind Farms

A study in SOWFA simulation environment

Master of Science Thesis

For the degree of Master of Science in Systems and Control at Delft University of Technology

Naveen Rajasekaran

July 9, 2020

Faculty of Mechanical, Maritime and Materials Engineering (3mE) · Delft University of Technology

Delft University of Technology
Department of
Delft Center for Systems and Control (dcsc)

The undersigned hereby certify that they have read and recommend to the Faculty of Mechanical, Maritime and Materials Engineering (3mE) for acceptance a thesis entitled

Towards Active Power Control of Waked Wind Farms

by

Naveen Rajasekaran

in partial fulfillment of the requirements for the degree of

Master of Science Systems and Control

Dated: July 9, 2020

Supervisor(s):

prof. dr. ir. J.W. van Wingerden

B.M. Doekemeijer

Reader(s):

prof. dr. ir. J.W. van Wingerden

Dr. R. Ferrari

Ir. B. Doekemeijer

Ir. T. Pippia

Summary

Wind energy is one of the most attractive solutions to help switch to a more sustainable way of energy production. The current decade has seen a steep increase in the installed capacity of wind turbines worldwide. This increasing trend in the installed capacity has put forth several challenges to maintain wind power as a profitable source of energy compared to other conventional energy resources.

The power generated from wind is not synchronized to the electrical frequency of the power grid. So grid balancing and reliability services have to be assured when the output from a wind farm is integrated into the electrical grid to avoid the risk of blackouts and disrupting electrical services. Active Power Control (APC) methods are employed to provide grid balancing ancillary services such as frequency control. One type of active power control method is the Automatic Generation Control (AGC), where the objective is to have the total power generated from a wind farm, track the power demand requirements obtained from the utility grid.

To be able to provide this kind of support, the wind farm should be able to operate below their maximum power production capacity i.e, in derating mode. The total power generated from the wind farm can track the demanded power reference signal, provided when each of the turbines in the wind farm can also be derated, and have the capacity to track their respective power setpoints. The amount of power that a wind turbine can generate depends on the wind speed that the turbine faces. The presence of wakes in the farm results in the downstream turbines in the wind farm to experience reduced wind speed and increased turbulence. So considering the presence of wake effect, a wind farm controller is developed to coordinate and distribute the overall power reference signal as set points to the individual turbine such that the sum of the power generated from the individual turbines tracks the total power reference signal.

Many model-based and model-free APC algorithms for wind farms are proposed in the literature. The model-based algorithms depended on the accuracy of the model used, and also were evaluated in a low fidelity simulation environment. But the researchers have also emphasized the need to test the algorithms in high fidelity models. Also, the earlier works on APC for wind farms revealed the need for a closed-loop wind farm control strategy to combat

the effect of wake turbulence. The presence of wakes posed several challenges on obtaining the estimate of the available power at every turbine on a time scale of seconds. Yet, some model-free algorithms were dependent on the estimation of available power at every turbine in the wind farm. This, leads us to the question, ***Can a wind farm controller be developed to provide APC for waked wind farms, where, the setpoint selection and distribution are made without estimating the available power at each turbine?***

To explore the answer to this question, a single wind turbine power tracking control algorithm is developed as the first step. This tracking algorithm does not depend on the estimation of available power and it makes an individual wind turbine in the wind farm to track a given power reference signal. The proposed algorithm makes the turbine operate on two different operating modes namely, the perfect tracking mode and greedy/boosting mode. The algorithms were developed in a way that they can be integrated with the existing torque and pitch controllers. The proposed algorithm was evaluated in a high fidelity model called as Simulator fOr Wind Farm Applications (SOWFA) for a two turbine case. The results of the simulation were promising as both the turbines were able to track their respective power references.

Following this, a closed-loop wind farm control strategy has been developed. The Proportional Integral (PI) based closed-loop wind farm controller takes the total power generated from the wind farm as the feedback signal. Based on the operating mode of the individual turbines, the wind farm controller coordinates and distributes the total power reference signal as individual power setpoints to the respective wind turbines. To determine the gains of the PI controller, the overall tracking performance of the wind farm controller is evaluated for varying controller gains, and the controller gain that leads to better tracking performance was finalized to be the gain of the controller.

The performance of the closed loop wind farm controller was evaluated for a 9 turbine case in SOWFA environment. Four different scenarios were simulated. They differed from each other based on the way the turbines in the wind farm are derated and the individual set points to the turbines are distributed by the wind farm controller. Simulation results showed that the scenario in which the upstream turbines in the wind farm are derated more than the downstream turbines, the tracking performance was better compared to the other scenarios. The Damage Equivalent Loads (DEL) experienced by the tower base of the individual turbines were also calculated and each of the scenario resulted in different loading patterns. In addition to this, recommendations are also provided to extend this work and perform further research.

Table of Contents

List of Figures

List of Tables

Acknowledgements

Firstly, I would like to thank my supervisor prof. dr. ir. J.W. van Wingerden for providing me this valuable opportunity to perform my thesis. At the same time, this work would not have been made possible without the support and mentorship of Ir. B. Doekemeijer, who was more than just a daily supervisor.

I extend my thanks to academic counsellor Lourdes Gallastegui for providing me the right support during the tough phases of my thesis.

Secondly, I thank my parents for being the pillar of support and a source of encouragement throughout this journey. Their constant prayers and love always pushed me further, whenever I got bogged down.

Thirdly, a special thanks to my friends, Pranav, Vinayak, Prasad, Krishna, Aditya and Nivas for all the support they provided me during my hard times. Life in Delft became more memorable and fun because of you guys being around.

Finally, I would like to thank TU Delft and the department of DCSC for providing a stimulated learning environment.

This journey has been nothing short of a roller coaster ride. At the end of this journey, I not only graduate with a master's degree but also graduate as a better human.

Delft, University of Technology | Naveen Rajasekaran
July 9, 2020

Dedicated to my Amma and Appa. This is for you.

Chapter 1

Introduction

Over-dependence on fossil fuels for power generation has caused environmental concerns over the years. Hence, there is considerable attention being given to alternative methods of generating power. Out of all the alternative sources of energy, wind is an inexhaustible resource which is available all over the world. The Secretary-General of World Wind Energy Association (WWEA), Stefan Gsänger emphasizes that,

"[...] The global transformation of the energy system towards renewable energy is on its way, and wind power is a major force in this development, having become a major pillar of power supply throughout the world. Some countries are making very good progress in accelerating wind power deployment rates. Such acceleration is imperative not only to achieve the objectives of the Paris Climate Change agreement and the Sustainable Development Goals but also for every country to participate in the full socio-economic advantages of renewable energy [3]."

As per the statistics released by the WWEA [1], by the end of the year 2019, the global wind power capacity has seen a growth rate of 10.1 % compared to the previous year. The worldwide installed capacity of wind turbines by the end of 2019, reached 601 Gigawatt as shown in Figure 1-2 . This enormous amount of increasing trend in the installed capacity has put forth several challenges to maintain wind power a profitable and competitive cost of energy compared to other conventional energy sources.

Wind energy is expected to be the largest source of energy in Europe by 2030 as the contribution of wind energy to electricity generation has increased multi fold in the past decade [5,58]. The deployment of large-scale offshore wind farms have been restricted due to the high costs of offshore wind energy as well as the utility grid balancing costs for the power output from an offshore wind farm [1]. However, with the advancements achieved in control methods, wind farms are now able to *provide grid balancing services as an ancillary service* apart from its main objective of *power maximization* [22] and *load optimization* [14].

[1]A wind farm is any group of wind turbines that acts together as a power plant and generate electricity. Offshore wind farms vary in size from a small number of turbines to several hundred wind turbines covering an extensive area in the sea as shown in Figure 1-1.

Figure 1-1: Part of the Gemini offshore wind farm located in the Netherlands. Picture taken from https://www.vanoord.com/sustainability/energy-transition/gemini-social-environmental-and-economic-spin

1-1 Active Power Control (APC) - an ancillary service

The power generated from the wind is not synchronized to the electrical frequency of the power grid. So grid balancing and reliability services have to be assured when the output from a wind farm is integrated into the electrical grid to avoid the risk of blackouts and distrupting electrical services [6, 19].

Active power control (APC) for an offshore wind farm is a control method to actively control the total power generated by the farm and balance it with the power consumed on the utility grid. With the advent of new economic policies worldwide [5], there need to provide market incentives for wind turbines to control their active power output and provide ancillary services such as frequency control [39] is on the rise. The contribution of wind power plants (WPP) in frequency support can be classified into

- **Inertial control:** Inertial control is the immediate response to a power disturbance event that occurs based on power supply-demand imbalance. During the initial instants of a frequency drop, in order to limit the rate of fall of frequency, wind farms can be used to provide inertial frequency support. For this, the kinetic energy stored in the rotor of the wind turbines are extracted [10, 17, 18].
- **Primary Frequency Control (PFC):** PFC is the response that follows the inertial control response. During the loss of supply or loss of load events, the power output of the generators are increased or decreased to balance the generation and load.

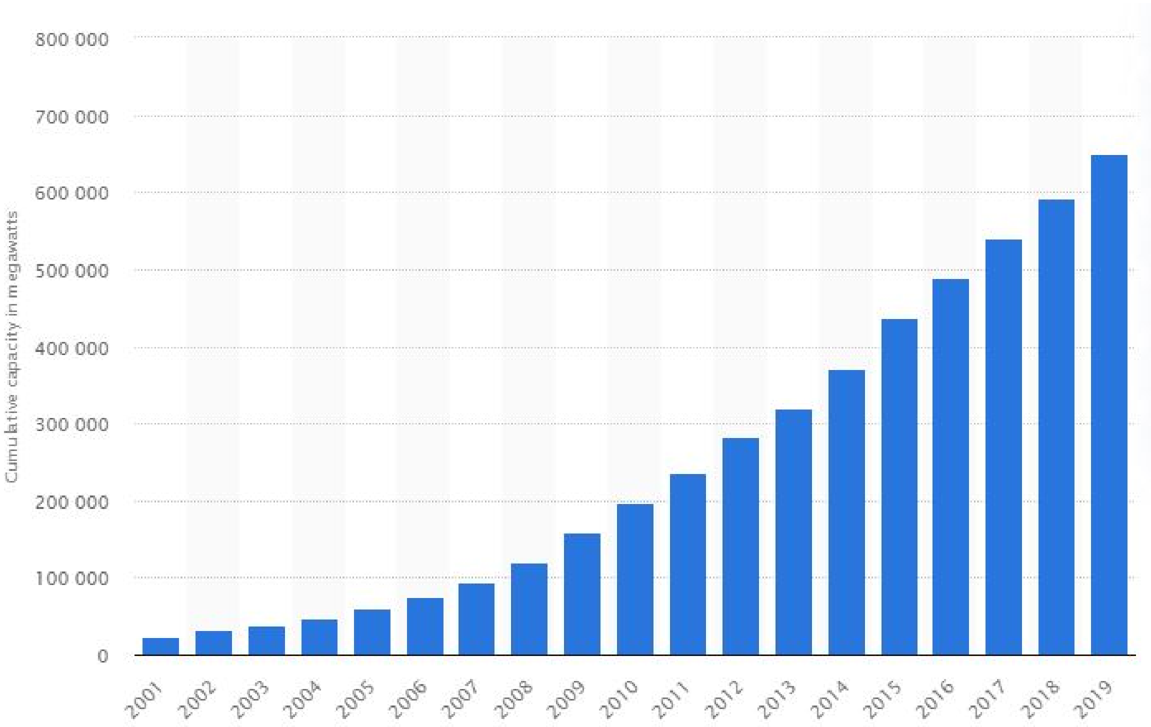

Figure 1-2: Global cumulative installed wind power capacity from 2001 to 2019 Picture taken from https://www.statista.com/statistics/268363/installed-wind-power-capacity-worldwide/

- **Automatic generation control (AGC):** In AGC, one of the objective is to have the power generated from the wind farm track the power reference signal generated by Transmission System Operator (TSO), during a span of several minutes [19]. To be able to provide this kind of support, wind farms should be able to operate below their maximum power production capacity i.e, in derating mode. *In this thesis, the focus is on the AGC method in which the wind farm should track a power reference signal provided by the TSO.*

1-1-1 Overview of active power control for a wind farm

A schematic showing the interconnection between the TSO, utility grid , the wind farm controller and the individual turbines can be seen in Figure 1-3. $P^{ref,tot} \in \mathbb{R}$ refers to the overall power reference command received by the wind farm controller. The predicted available power of the entire wind farm, $P^{a,tot} \in \mathbb{R}$, is communicated back to the TSO by the wind farm controller. The wind farm controller distributes the overall power reference signal as set points to the N individual turbines in the wind farm, $P^{dem} \in \mathbb{R}^{N_T}$. $P^{a} \in \mathbb{R}^{N_T}$ denotes the estimate of the available power at every turbine. The wind farm controller distributes the set points based on this estimate. Each individual turbine in the farm is equipped with a pitch control and a torque control system that controls the power generated out of the turbine.

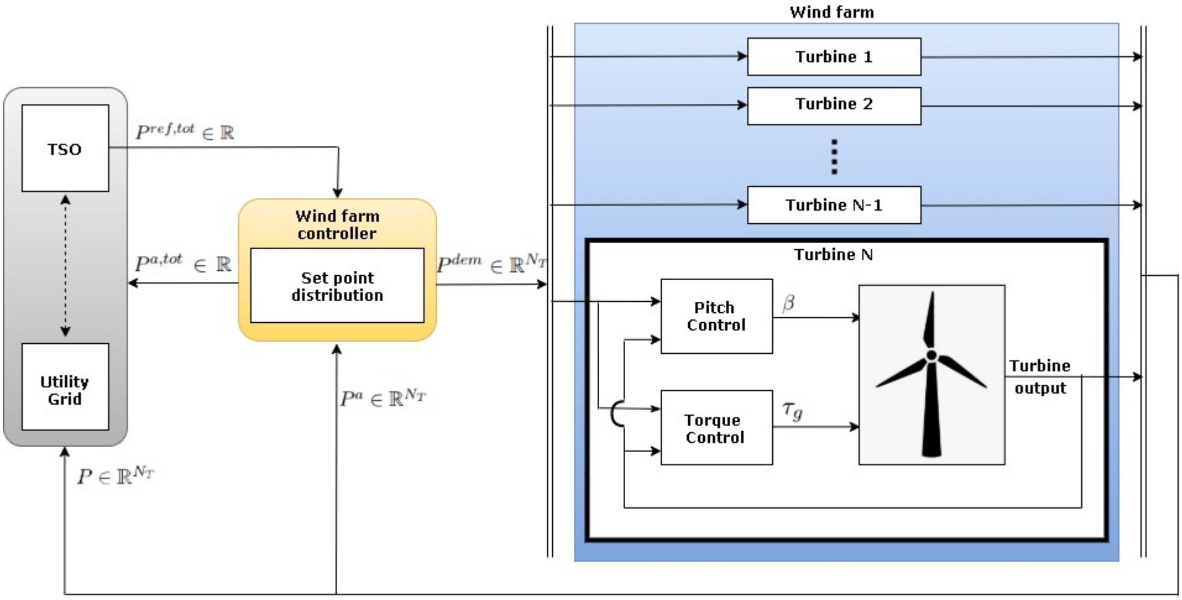

Figure 1-3: A schematic representation giving an overview of the wind farm controller showing the interconnections and signal flows involved between the TSO, utility grid, wind farm controller and individual turbines inside a wind farm.

1-1-2 The wake challenge

When APC has to be provided for a wind farm, the wind turbines in the farm, are coordinated to generate power to match the demand from the utility grid. The maximum power that the turbines in a wind farm can generate depends on the wind speed faced by each turbine. Within a wind farm, when a wind turbine extracts energy from the wind. The wind flow in the downstream of that turbine changes. The change in the wind flow is called the wake of a turbine. Wakes lead to increased turbulence and reduction of wind speed faced by the downstream turbines. Hence, the development of APC for a wind farm should consider the effect of wakes as well. Studying and modeling the wake behaviour is a separate research topic by itself and that is out of the scope for this thesis. To maximize total power generation and minimize the power losses caused by the wakes, several strategies have been proposed in the literature. Some of them are based on redirecting the wakes around the downstream turbines by yawing or tilting [9, 23, 43, 55] the wind turbines and the others are based on the redistribution of power contribution of each turbine [47, 49]. In this thesis, the works related to the latter are only considered.

1-2 Previous work on APC for wind farms

In recent years, significant amount of research have been published related to active power control for wind farms. Researchers have proposed and analysed different APC algorithms [6, 7, 11–13, 21, 25, 27, 32, 38, 44, 48, 52–55, 57]. Some significant ideas and excerpts from some of those literature will be presented in this section.

The early works of implementing APC control for a wind farm was demonstrated by Fleming et al. [21]. In this paper, an open loop supervisory controller coordinates the turbines by derating them and evenly distributing the power set point requirements to the individual turbines. A Computational Fluid Dynamics (CFD) simulation study was done for a low waking and a high waking case. Although the open loop controller managed to yield very good power tracking performance for the low waking case, the performance of that controller proved to be unacceptable in case of high wake interaction.

To overcome this problem, a simple, model free closed loop solution was developed by van Wingerden et al [58]. Set point distribution to the individual turbines were done based on an estimate of the available power at every turbine. The author also pointed out the estimation of available power at every turbine is a challenging task because of the largely unpredictable nature of wind at a faster timescale. Thus to avoid that uncertainty, the wind farm power measurement was taken as the feedback and a simple Proportioanl Integral (PI) based closed loop controller was developed. The controller proved to be stable and very effective in improving the wind farm behaviour in the presence of wake interaction between the turbines. The performance of this closed loop wind farm controller was evaluated for a 9 turbine case arranged in a 3×3 grid, by using the high fidelity model - Simulator fOr Wind Farm Applications (SOWFA) tool which has a Fatigue, Aerodynamics, Structures, and Turbulence (FAST) wind turbine simulator coupled to it for computing the dynamic response of wind turbines. The simulations were performed for two different scenarios. In the first scenario (Case: 50-50-50), every turbine was derated to 50% of the rated power and in the second scenario (Case: 80-50-20), the first row of turbines was derated to 80%, the second row to 50% and the last row to 20%. The results showed that there exists disparate loading patters on the wind turbine components, for the case where the power set points were determined differently.

Siniscalchi et al. [48] proposed a control strategy to maximize the power reserve in the wind power plant while satisfying the power demand requirements. An optimization procedure was developed to distribute the set points to individual turbines. The proposed strategy reduces the power contribution from the upstream turbines such that the downstream turbines face increased wind speeds resulting in higher available powers. Simulations were performed in a relatively simple AEOLUS SimWindFarm (SWF) Simulink toolbox for a 12 turbine case. The proposed set point distribution strategy proved to perform better when it was compared with the case where the set points were distributed proportional to the available powers at each turbine. The effect of the proposed power maximization strategy on the mechanical loads were not studied in this work and also the author has emphasized the need to test the proposed algorithm in a high fidelity simulation environment.

Apart from the model free approaches, researchers have also developed model based APC solutions recently. Model Predictive Control (MPC) based solutions for optimal distribution of power reference to the individual turbines in the farm by taking wake interactions into consideration can be found in [32, 46, 52].

Zhao et al. [60] proposed an MPC based solution for providing APC for wind farms. This method had a high level controller to distribute power commands and a low level MPC based wind farm controller that operates on a higher frequency when compared to that of the high level controller. Although the proposed controller managed to reduce the fluctuations in the power output and reduce structural loads, the proposed solution had its limitations because of its open loop characteristics.

Another MPC based solution to reduce structural loads has been presented in [44]. However, reducing computational complexity of MPC based solutions is still an open research topic for large wind farms [52]. Bay et al. [11] developed a distributed MPC based solution that reduces the computational complexity by limiting the communication among the turbines in wind farm.

1-3 Problem statement and thesis objectives

Looking at the previous work done on APC for wind farms in section 1-2, the following points can be inferred.

- To make the total power output of the wind farm track a demanded power reference signal, an overall wind farm controller must coordinate the power set points of the individual turbines in such a way that the power produced from the individual wind turbines sums up to the desired amount. The coordination of set points becomes complicated because of the presence of wakes.
- The set point distributions were done based on the estimate of the available power. It is a challenging problem considering the unpredictable nature of the wind and hence the estimation of available power at a faster time scale becomes difficult.
- A closed loop wind farm control strategy is necessary to compensate for the uncertainty in the estimation of available power and thereby redistribute the set points to the turbines to address the under-performance of some turbines due to the lulls.
- Many wind farm controller studies have proposed various methods for active power control and verified the performance through simulations. They have limitations because simple wind turbine models are only used in their simulations. A better insight about the performance of the control strategies developed for waked wind farms can be obtained when the controllers are evaluated in a high fidelity simulation environment.
- Model based methods require accurate models and also most of the model based methods for wind farm APC were simulated using low fidelity models. Hence, model free methods only will be considered for the thesis.

Considering the inferences mentioned above and also the drawbacks realized from the literature as discussed in section 1-2, leads to the following questions which can be the problem statements under consideration for this thesis.

- ***Can a wind farm controller be developed to provide APC for waked wind farms, where, the set point selection and distribution are happen without estimating the available power at each turbine?***
- ***How do different set point distributions affect the tracking performance of the controller and how does the load experienced by the turbines differ based on different set point distribution scenarios?***
- ***How is the tracking performance affected when the gains of the wind farm controller are changed?***

1-3-1 Objectives of the thesis

The objectives of the thesis are framed based on the problem statements under consideration.

- First, a control system that commands an individual wind turbine to track a given power reference set point is developed.
- Second, a wind farm controller that considers the operating mode of the individual turbine to distribute the power set points such that the total power output of the wind farm will be made to follow the demanded power signal is developed.
- The performance of such a controller is evaluated under different set point distribution scenarios and the damage equivalent loads of individual turbines are evaluated and compared for the respective scenarios

All the simulations will be performed in a high fidelity simulation environment for a 9 turbine waked wind farm.

1-4 Outline of the thesis

Apart from the introduction chapter, this thesis has 4 more chapters and the chapters are divided as follows.

- Chapter 2: The preliminaries for understanding a wind turbine control system is described. Following that the development of the control system that enables the wind turbine to track a given reference is proposed and discussed. Finally, the performance of the proposed controller is evaluated with a simulation study for a 2 turbine case.
- Chapter 3: The wind farm control development procedure to that coordinates all the turbines in the given wind farm and makes the total power output of the wind farm follow a demanded trajectory is discussed.
- Chapter 4: To evaluate the proposed wind farm controller, different scenarios for set point distributions are considered. The way in which the simulations are set up for a 9 turbine wind farm case is discussed in the beginning . Following that, the performance of the controller is evaluated and discussed for the respective scenarios.
- Chapter 5: The concluding points of the thesis are given. Following that the recommendations for future research are also suggested.

Chapter 2

Single wind turbine power reference tracking control

In the introduction chapter, we saw about the importance of active power control algorithms and how they are used to enable a wind farm to deliver the power levels demanded by the TSO. The main task of an active power controller for a wind farm is to adequately distribute the total wind farm power reference over the individual wind turbines such that the total power generated from the wind farm, obtained by the sum of power generated from individual turbines tracks the power reference. This is possible only when the turbines in the wind farm are able to track a given power reference. A typical wind turbine can be made to track a power reference by means of derating i.e, by lowering the power output of individual turbines [44] [6]. In this chapter, we will see about the development of a single wind turbine control system that enables the turbine to track a given power reference. In Section 2-1, a brief overview is provided about traditional wind turbine control system. The relevant works done previously with respect to the development of a single wind turbine reference tracking control are discussed in Section 2-2. In Section 2-3, a method to derate a single wind turbine to make it track power set point is proposed. In Section 2-4, the proposed algorithm is tested and evaluated by using a high-fidelity simulation model for a 2 turbine case .

2-1 Wind turbine as an energy source

Majority of the large scale wind turbines today are Horizontal Axis Wind Turbine (HAWT). These turbines are operated in an upwind manner [5]. When wind passes over the blades of the turbine, it produces a lift force and this induces a rotational torque.

For a uniform wind field, if ρ is the air density and ν is the wind speed passing through the swept area A of the rotor disk, then the power in that uniform wind field is given by

$$P_a = \frac{1}{2}\rho A \nu^3$$

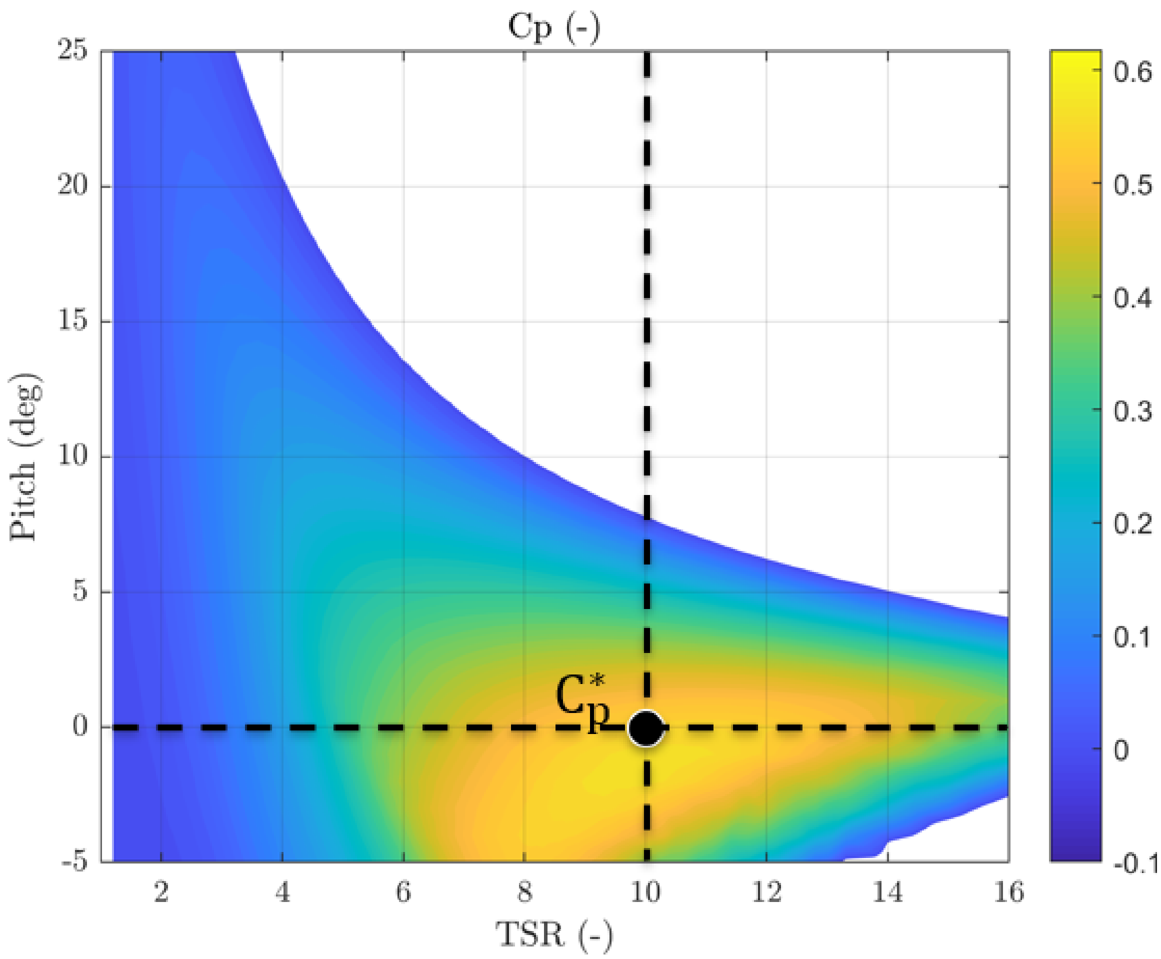

Figure 2-1: A characterization of the power coefficient C_p of the NREL 5 MW wind turbine. The black line represents the TSR λ_* and the collective pitch angle β_* resulting in the optimal power coefficient C_p^*

.

The wind turbine can only capture a fraction of the power in the wind. The ratio of the power captured by the turbine to the power in the wind is given by $C_p(\beta, \lambda)$, also referred as the power coefficient. C_p is a function the collective pitch angle β and the Tip Speed Ratio (TSR) λ . A characterization of the power coefficient C_p for the wind turbine used in this study is shown as a contour plot in Figure 2-1.

Tip Speed Ratio (λ) is defined as the ratio between the tangential speed of the tip of a blade and the actual speed of the wind. This is given by, $\lambda = \frac{\omega_r R}{\nu}$, where R is the rotor radius and ω_r is the rotor speed.

The aerodynamic torque captured by the blade is transferred to the hub of the turbine, which connects the blades to the generator through a drivetrain system. The wind turbine's generator converts the mechanical power of the drivetrain to electrical power which is either directly injected to the grid or first converted to the grid frequency via power electronics.

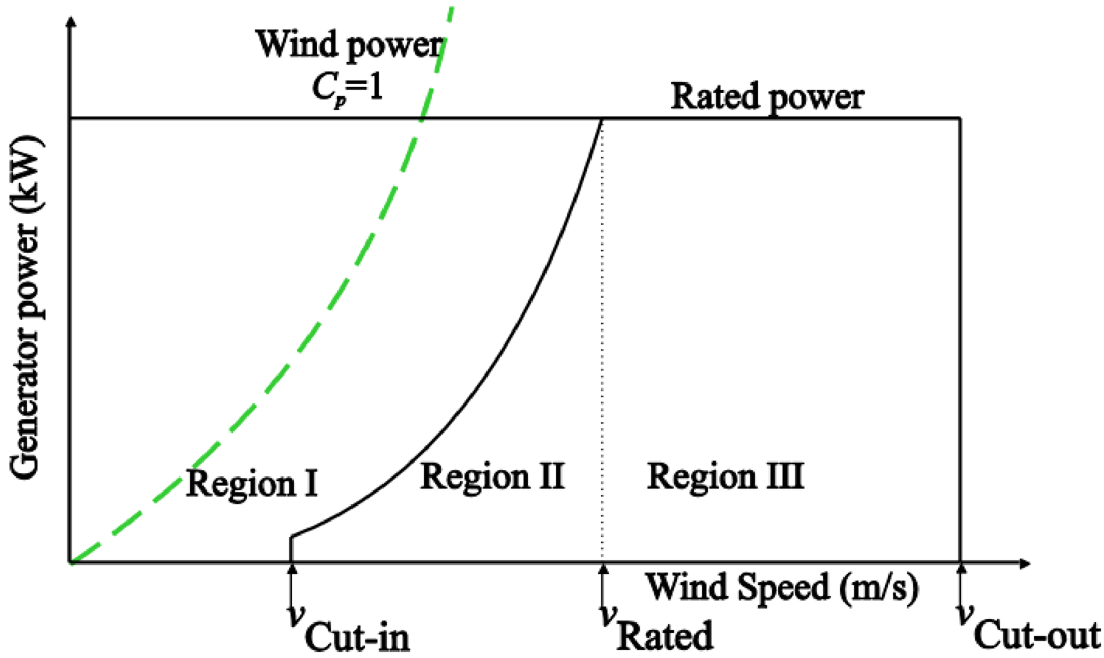

Figure 2-2: Wind turbine operation regions [41]

2-1-1 Operating regions and control of wind turbines

The primary goal of traditional wind turbine control system is to *maximize the energy capture and minimize the structural loads* [6]. The focus of the control objectives differ depending on the operating regions of the wind turbine, which is usually divided into three regions as shown in Figure 2-2.

- **Region I:** Below the cut-in speed is the Region I. Here the wind speed is too low for the operation of the wind turbine.
- **Region II:** The region between the cut-in wind speed and the rated wind speed is Region II. The primary objective of the wind turbine operated in this region is maximizing the amount of power extraction. In standard Region 2 control, the goal is to maintain the TSR at the optimal level λ_*. By holding the collective blade pitch angle at a constant value β_*, the generator torque is varied to achieve TSR value as λ_*. Thereby, the turbine is made to operate at the maximum C_p value. This is called as the **generator torque control**. If ω_g is the generator speed, then the generator torque controller works on the law given by,

$$\begin{aligned} \tau_g &= K_T \omega_g^2 \\ K_T &= \frac{\rho \pi R^5 C_p(\beta_*, \lambda_*)}{2\lambda_*^3} \end{aligned} \tag{2-1}$$

- **Region III:** In above-rated wind conditions (Region III), the idea is to mitigate loads on the mechanical structure and on the power electronics by limiting the power capture.

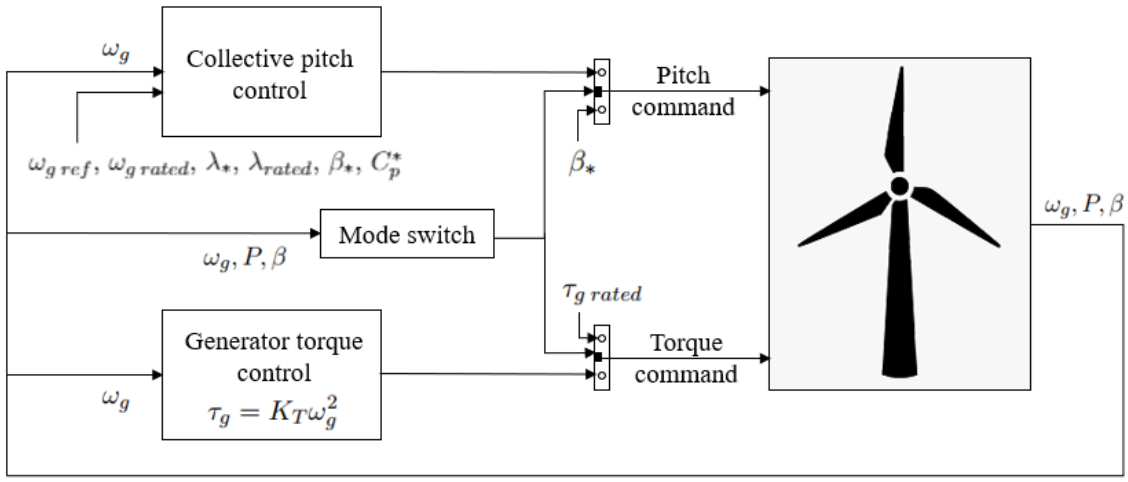

Figure 2-3: Traditional wind turbine control system

To regulate the generator speed and make the turbine operate at the rated speed value, the ***blade pitch controller*** is used. Here the pitch angle (β) of each blade is collectively adjusted by the same amount in response to the rotor speed measurement. This is called Collective Pitch Control (CPC) [36]. This is traditionally done by holding the generator torque constant so that the generator speed (rotor speed) is at the rated value. The blades of the turbine are pitched to sub-optimal conditions, thereby purposely deviating from the optimal $C_p(\lambda_*, \beta_*)$ [41]. A standard collective blade pitch control system uses proportional integral (PI) control. This PI controller regulates the generator speed to the rated value by acting on the generator speed error signal.

- When the wind speed is above the cut-out wind speed and the wind turbine is shut down by supervisory control. This is termed as the Region IV.

Figure 2-3 shows the schematic block diagram of the traditional wind turbine control system having torque and pitch control loop. The torque controller block functions on the control law as shown in equation 2-1 and that mode is switched on when the turbine is operating for power maximization in the below rated condition. The pitch value is maintained at the fine pitch angle β_*. When the power generated from the turbine reaches the rated power or when the available power in the wind reaches the rated value, the torque is maintained at $\tau_{g\,rated}$ and then the collective pitch control loop is switched on. The mode switch uses the information on generator speed, blade pitch angle and power output from the turbine and their respective rated limit values to enable the right control loop.

2-1-2 Need for derating the turbine for power reference tracking?

The power generated by the wind turbine is $P = \frac{1}{2}\rho A C_p(\beta, \lambda)\nu^3$. For maximizing the power production, the torque controller aims to track the optimal power coefficient C_p^* until the power produced by the turbine reaches rated power. As C_p being a function of TSR and pitch angle, the rotor speed is controlled through the generator torque such that the turbine operates in the desired optimal TSR value to maximize the power produced. In simple words, the torque controller in equation 2-1 tries to track the optimal C_p everytime to produce maximum power. When the turbine is demanded to produce certain amount of power so as to track the demanded power command from a higher level wind farm controller, the traditional wind turbine control system is incapable of doing that. Tracking a power command by derating the turbine is to track a sub-optimal C_p value. Hence efforts have been made to develop control algorithms to track sub optimal C_p and thereby achieve demanded power tracking by means of derating the turbine.

Some of the significant algorithms developed earlier will be discussed in in section 2-2 to understand the general approach followed by the researchers. Drawing inspiration from the that, a new algorithm for a single turbine power tracking control will be proposed and discussed in section

2-2 Previous work on single wind turbine power reference tracking control

Aho et al. [6] developed the a wind turbine control system which actively controls the power output of the turbine to track power set point commands. The algorithm derates the turbine by operating it at a TSR value that is higher than the optimal TSR value and thereby the kinetic energy on the rotor is stored which can be used to provide primary frequency response. The power tracking is achieved by scheduling the K_T value in the torque feedback law (equation 2-1) according to the power set point commands and also by adding the low pass filtered component of primary power reference command to the derating commands. The scheduling of the power commands were dependent on the estimate of power that the turbine could theoretically capture when the turbine is operating at the maximum power coefficient. As the algorithm is majorly based on accurate scheduling of the gain value, the accuracy of the turbine model used gains importance. Providing a primary frequency response with a droop curve slope also resulted in the increase of damage equivalent loads. The estimator used for obtaining the wind speed estimate also had issues with potential instabilities and bandwidth limitations.

Jeong et al. [28] developed and compared 5 different APC algorithms. The algorithms that used generator torque dominantly for control seem to have faster response and they are used for storing more kinetic energy in the rotor. The torque based algorithm provided faster performance but performed better only in the above rated region. The performance was undesirable in region II because of excessive increase in rotor speed. The algorithms that used blade pitching dominantly showed less loading. The algorithms were tested by simulations in FAST [30]. A field test was also performed on a 550 KW wind turbine with the algorithm that performed the best across (pitch control 2) a full range of turbine operations in terms of power tracking error. The field test results were significantly different from the simulation. Hence, the authors concluded that a method which integrates the pitch control 2 algorithm along with the torque based APC might be the ideal strategy to achieve power tracking performance over all wind speeds.

Kim et al. [34] developed 2 control algorithms (KNU1 and KNU2) for demanded power tracking for a single wind turbine. The first algorithm uses the generator torque with fixed blade-pitch angle. The KNU2 algorithm used the generator torque and the pitch control combination to achieve the power tracking. The two algorithms were developed in such a way that they can be integrated with the standard torque and pitch controller. The algoirthm was experimentally by performing a wind tunnel test. The first algorithm performed faster in tracking the power commands than the other algorithm. The second algorithm had advantage with respect to the loads. The paper lacked the description about the method to extract the kinetic energy stored in the rotor which can used for providing inertial response (boosting).

Modern control algorithms with multi input multi output (MIMO) controllers were also proposed to achieve power tracking [26, 59]. But, such methods are not considered for this thesis.

Looking at the above references in this section, the following can be observed and inferred.

- Most of the algorithms that have been developed for power tracking control use the combination of generator torque and pitch to achieve the control objective. The researchers have tried to integrate their proposed algorithm into the traditional wind turbine control structure itself for simplicity.
- Except from [6], the other works lacked description of methods to extract kinetic energy stored in the rotor.
- As stated in [56], tracking a power command by derating is equal to tracking a sub optimal C_p value. The shape of the C_p curve changes with respect to changing wind speeds and also to track the demanded power command, the prior knowledge of the incoming wind speed, available power and TSR values corresponding to the target C_p values becomes necessary information for the development of tracking controller.
- The turbine controller algorithm developed in [6] used the estimate of available power to develop the scheduling of derating commands. As stated in Section 1-3, the estimation of available power posed several challenges in the design of farm controller in terms of set point selection and distribution. So developing a single wind turbine power reference tracking algorithm dependent on estimation of available power will create further challenges.

Considering the inferences, the drawbacks from the relevant literature mentioned in Section 2-2 and also the objectives of this thesis, an algorithm for power reference tracking for a single wind turbine that can be integrated into the traditional wind turbine control structure and also which doesn't depend upon the estimation of available power has been proposed in the next section.

2-3 Development of single wind turbine power reference tracking controller

The main goal of this controller is to enable the wind turbine to track the power commands. The turbine can be commanded to generate a particular percentage of the demanded power or can be commanded to operate in the greedy mode to generate the maximum possible power that is currently available. The maximum power that can be demanded from the turbine is upper bounded by the rated power of the wind turbine.

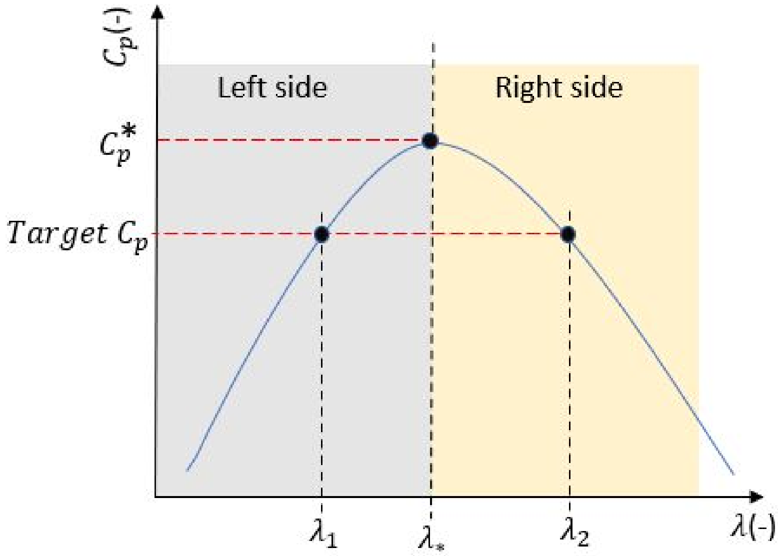

Figure 2-4: Illustration of $C_p - \lambda$ curve for a given wind speed and pitch angle. Left side and right side of the C_p curve are indicated with different shades. C_p^* is the optimal power coefficient. The two TSR values corresponding to the target sub-optimal C_p are indicated as λ_1 and λ_2 on the left and right hand side of C_p curve respectively.

2-3-1 Considerations for the controller development

The objective of tracking a sub-optimal C_p can be achieved by operating the turbine in two different TSR values , thereby two different rotor speeds. Referring to the illustration shown in Figure 2-4, for a given wind speed and pitch angle, the turbine can either be operated on a TSR value that is lower than the optimal TSR (λ_*) (on the left hand side of the C_p curve) or on a TSR value that is higher than λ_* (on the right side of the C_p curve).

To operate the turbine on the left side of the C_p curve, a torque value that is higher than the torque required to make the turbine to operate at the optimal TSR (τ_g) is required. But, to operate on the right side of the C_p curve less torque is needed than τ_g. Higher torque leads to slowing down of the rotor speed and vice versa. Hence operating on the left side of the C_p curve leads to further slowing down of the turbine rotor speed. This is an undesirable behaviour and it leads to stability issues [31, 35, 40].

Hence, tracking a sub-optimal C_p can be achieved by making the turbine operate at a higher TSR (higher rotor speed). Such a method has been presented in [6, 31, 37, 56]. The advantage of operating the turbine at higher rotor speed is that more kinetic energy can be stored in the rotor and that kinetic energy can be extracted to provide inertial response or boosting whenever required.

Operating at higher rotor speed can also have some disadvantages. According to van der Hoek et al [56], the turbines experience maximum thrust force when operated at rated rotor speed and the thrust force decreases when the pitch controller is activated. For an entire wind speed range, the thrust force can be computed as , $T = \frac{1}{2}\rho C_T A \nu^2$. Here, ν refers to the wind speed and C_T refers to the thrust coefficient of the wind turbine. Figure 2-5 shows the contour plot of the thrust coefficient of the wind turbine for a given wind speed. As operating

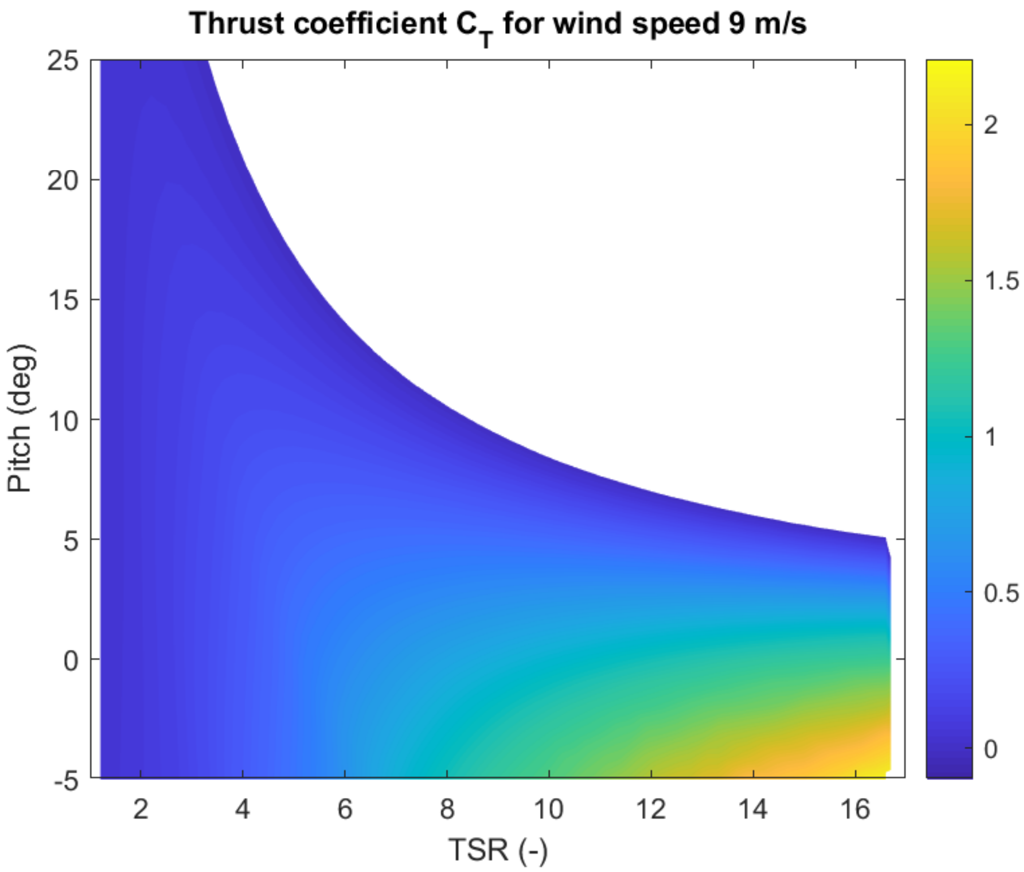

Figure 2-5: Contour plot of the thrust coefficient C_T

the turbine at lower TSR reduces the thrust coefficient (C_T), reducing the maximum rotor speed would result in larger decrease in thrust force. This also prevents the formation of deeper wakes [4, 24].

For the purpose of reducing the maximum rotor speed, TSR limits are defined. Corresponding to the defined TSR limits, the rated rotor speed limit zone is calculated for for a given wind speed. This zone is termed as the up-spin zone. The collective blade pitch angle is adjusted in such a way that the turbine rotor speeds up and operates within the defined TSR limits. This pitch angle adjustment is also necessary to prevent the wind turbine rotor from over-speeding and also prevent the operation of turbine in the stall region.

Figure 2-6 shows the block diagram of the proposed controller for demanded power tracking. The controller has three main blocks namely the wind speed estimator, torque controller, the collective blade pitch controller. The controller has two different operating modes namely the perfect tracking mode and greedy/boosting mode. Each of the three blocks and the two operation modes will be described below.

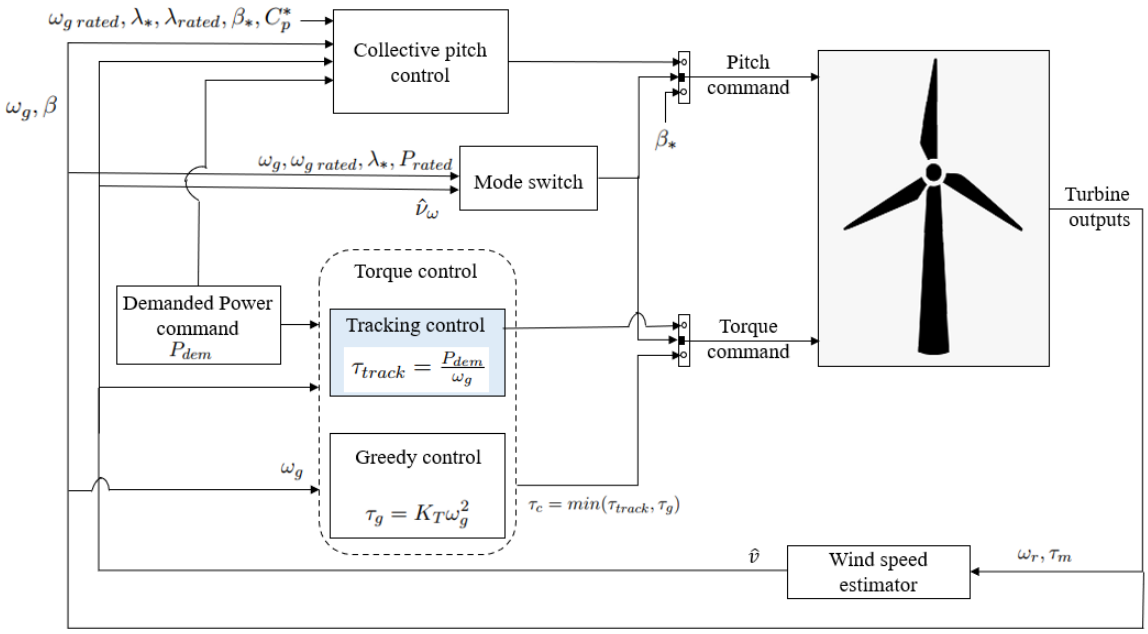

Figure 2-6: Demanded power reference tracking controller

2-3-2 Wind speed estimator

With the objective to track a sub-optimal C_p, the prior knowledge of wind speed will enable the wind turbine controller to determine the current operating point on the C_p curve and thereby apply required control action to reach the targeted sub-optimal C_p. Hence, we use a wind speed estimator for this purpose.

Several wind speed estimation strategies have been proposed by the wind speed community. Soltani et al. [50] compared different wind speed methods namely power balance estimator, Extended Kalman Filter (EKF) based estimator, Kalman Filter (KF) based estimator, Disturbance Accommodating Control (DAC), Unknown Input Observer (UIO) and Immersion and Invaraiance (I&I) estimator. The author compared simulation and field test results to conclude that the I&I estimator performed better in all turbulence intensities and it is simpler for implementation as it does not require linearization of C_p table for the estimator to be designed.

Hence in this thesis, the **I&I estimator** concept will be used to design the required wind speed estimator.

The design of the I&I estimator is based on the work done by Ortega et al. [42]. The design is based on the assumption that the measurement of rotor speed and electrical torque are available. In that paper, the dependence of pitch angle β was excluded in the design steps and stability proofs of the estimator because the estimator's intended region of operation was only in Region II.

I&I estimator

The controller that is intended to be developed for power tracking in this thesis, requires the estimator to operate on the full wind speed range. Hence, the design of the I&I estimator needs to be done considering the dependence of pitch angle.

Although, the dependence of pitch angle is omitted in the work done by Ortega et al., it has been mentioned in the paper that including the pitch signal into the estimator design will not affect the estimator derivations.

Deriving the estimator design steps and proving stability of the estimator when pitch angle is included into the design is not considered in the scope of this thesis work. However, the empirical results through simulations demonstrated that the estimator performance is stable for the entire wind speed range.

The implemented *I&I* estimator equations to determine the wind speed estimate is given by,

$$\begin{aligned} \dot{\hat{\nu}}^I &= \gamma \left[\frac{\rho A (\hat{\nu}^I + \gamma \omega_r)^3}{2\omega_r} C_p \left(\frac{r\omega_r}{(\hat{\nu}^I + \gamma\omega_r)}, \beta \right) \right] \\ \hat{\nu} &= \dot{\hat{\nu}}^I + \gamma \omega_r \end{aligned} \tag{2-2}$$

Here, $\hat{\nu}$ is the estimate of the wind speed ν
ω_r is the rotor speed
$\gamma \geq 0$ is an adaptation gain (tuning parameter) which can be tuned to achieve the desire convergence speed of estimation and noise filtering.

The estimate asymptotically converges and becomes,

$$\lim_{t \to \infty} \hat{\nu}(t) = \nu$$

2-3-3 Collective blade pitch controller

The collective blade pitch controller used in this work, differs from the standard gain scheduled PI controller as described in [29] [6]. This controller ensures to pitch the blades in such a way that over-speeding of rotor is prevented and also ensures that the rotor speed doesn't exceed the rated rotor speed limits. The blade pitch angle is lower bounded by the fine pitch angle β_* (0°).

The blade pitch controller here is a simple function that considers the measured generator speed, rated rotor speed limits, TSR rated limits, Pitch limits and the corresponding interpolated C_p values to evaluate the pitch angle β required to maintain the rotor speed at the within the rated rotor speed limits and thereby enable the tracking of targeted sub-optimal C_p.

To achieve this, collective blade pitch controller compares the measured rotor speed with the lower limit and the upper limit of the rated rotor speed limits. If the measured rotor speed is less than the lower limit of the rated rotor speed limit values, then the controller commands the fine pitch angle β_* (0°). Else, if the measured rotor speed is greater than or equal to the upper limit of the rated rotor speed limit values, then controller commands out a pitch angle in the following manner.

Firstly, the targeted sub-optimal C_p value is determined based on power set point and the available power for the instantaneous wind speed. Corresponding to the targeted C_p value, the collective blade pitch angle that enables the turbine to operate on the right side of the C_p curve and also maintain the rotor speed within rated rotor speed limits gets determined.

2-3-4 Torque controller

The torque controller has two sub blocks.

- One of the sub-blocks operates on the greedy control law where the objective is to generate maximum possible power at that wind speed. The controller commands out a generator torque τ_g as per equation 2-1 by regulating the generator speed ω_g and operating the turbine at the optimal power coefficient $C_p(\lambda_*, \beta_*)$.
- The other sub-block operates based on the perfect tracking law. As, power is equal to torque multiplied by rotor speed, the tracking law is given by,

$$\tau_{track} = \frac{P_{dem}}{\omega_g} \tag{2-3}$$

  This means that for a given power demand signal, the controller commands out the torque τ_{track}, by adjusting the generator/rotor speed to the desired value such that power generated from the turbine perfectly tracks the reference power command.

2-3-5 Operational modes

The mode switch operation here differs from the traditional wind turbine controller. The mode switch here, uses the measurements from the turbine and the estimated wind speed to enable or disable, the tracking law and collective blade pitch control at the same time. In other words, the tracking law and the collective blade pitch control system acts together to achieve demanded power tracking.

Perfect tracking mode: In perfect tracking mode, the controller enables the tracking law and the collective blade pitch controller together. The controller commands the torque τ_{track} (as given in equation 2-3) and the collective pitch angle such that the rotor speeds up and the turbine operates within the defined TSR limits. Thereby, with the combination of the torque command and collective blade pitch angle adjustment, the tracking of the targeted sub-optimal C_p is achieved.

Greedy/boosting mode: In this mode of operation, The collective pitch angle is maintained at the fine pitch angle β_* and the the controller commands the generator torque τ_c which is equal to the minimum of τ_{track} (equation 2-3) and τ_g (equation 2-1).

$$\tau_c = min(\tau_{track}, \tau_g) \tag{2-4}$$

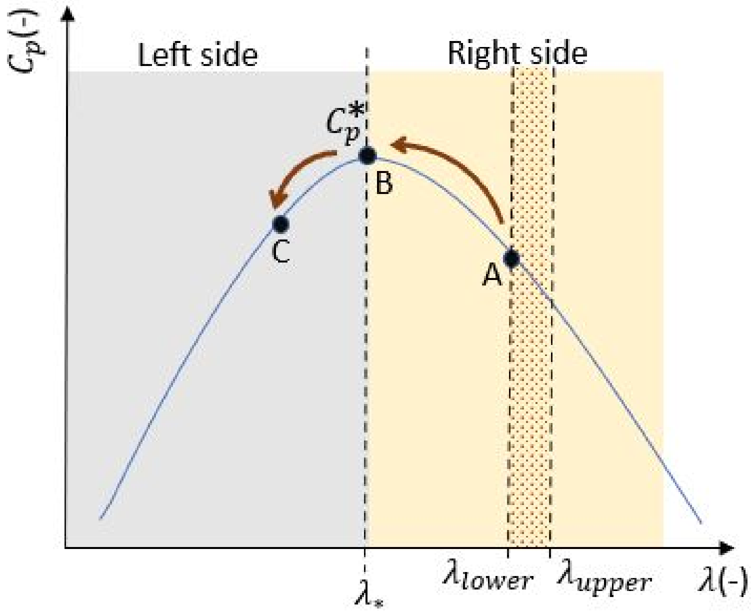

Figure 2-7: Illustration of $C_p - \lambda$ curve for a given wind speed and pitch angle at β_*. Points A, B and C represents different operating points of the turbine. The up-spin zone is marked with respect to the TSR limits λ_{lower} and λ_{upper}.

To understand equation 2-4 better, let us take a look at the illustration of $(C_p - \lambda\ )$ curve at β_* shown in Figure 2-7. When the turbine is operating on the right side of C_p curve, the rotor speed of the turbine is higher when compared to the optimum rotor speed ω_* at C_p^*. The rotor speed is further lower when the turbine is operating on the left side of the C_p curve.

The torque required to make the turbine operate at point A is less than that of the torque required to make the turbine operate at point B which is at the C_p^*. This implies that if the turbine's operating point has to be shifted from point A to point B, the demanded torque needs to be increased and this makes the rotor to down spin (slow down) to reach the rotor speed ω_*. Hence reaching point C (left side of C_p curve) from point B means that the demanded torque further increases leading to further slowing down of the rotor. As discussed in Section 2-3-1, this is an undesirable behaviour and it leads to stability issues.

Hence, when the blades are pitched at fine pitch angle and whenever the controller commands the torque $\tau_c = \tau_{track}$, the rotor slows down (TSR decreases) and the kinetic energy stored in the rotor is extracted to enable perfect tracking of the demanded power until the TSR value reaches λ_* (rotor speed reaches ω_*). This way of extracting the kinetic energy from the rotor to allow perfect tracking to happen is termed as the boosting mode.

When the commanded generator torque $\tau_c = \tau_g$, it is called as the greedy mode of operation. In this mode, the controller ensures that the commanded generator torque is never greater than τ_g. By this way, slowing down of the rotor further is avoided, when measured rotor speed is already on the left side of the C_p curve. Thus, in greedy mode the turbine operates at C_p^* and generates maximum possible power at that wind speed.

In simple words, the generator torque required to make the turbine operate in boosting mode is less than that of the torque required to make the operate the turbine in greedy mode. This explains the presence of *min* operator in equation 2-4.

2-3-6 Controller working method

Based on the power command received P_{dem} and the current estimate of the wind speed, the controller calculates the target C_p value for doing the perfect tracking.

The controller checks if the current rotor speed is on the right side of the C_p curve (current rotor speed is greater than the optimal rotor speed ω_*) and if it is greater than or equal to the upper limit of the rated rotor speed limit zone. If so, the turbine goes into the perfect tracking operational mode where the combination of torque command τ_{track} and collective blade pitch angle adjustment ensures that the rotor speed is maintained within the speed limit zone and eventually the targeted C_p value is tracked.

If the current rotor speed falls below the lower limit of the rated rotor speed limits, the mode switch disables the perfect tracking operational mode and enables the greedy/boosting operational mode. The controller commands to reduce the pitch angle to fine pitch (β_*) and then applies the generator torque τ_{track} such that the perfect tracking is still achieved by extracting the kinetic energy stored in the rotor until the rotor spins down to reach the optimal rotor speed ω_*. The controller then commands the generator torque τ_g such that the rotor speed is regulated at ω_* and the turbine is operated at C_p^*.

2-4 Simulation and analysis

To evaluate the performance of the proposed single wind turbine power reference tracking controller, a 2 turbine case study is performed. The wind turbines are placed one behind the other such that the second turbine is under the influence of wake created by the first turbine. Each of the turbine is demanded to track a particular percentage of the total power reference signal and the tracking performance of each of the turbine is discussed.

2-4-1 Simulation set up

To evaluate the proposed controller for power tracking, we use the high fidelity model - Simulator fOr Wind Farm Applications (SOWFA) that was developed by the National Renewable Energy Laboratory (NREL). For further explanation of this simulation tool, refer section 4-1 in chapter 4.

NREL 5 MW reference turbine is considered for the simulations in SOWFA. Two turbines (WT1 and WT2) are considered for the study and are placed at a distance of 5D where D represents the rotor diameter as shown in Figure 2-8(a). Simulations are performed with wind speed of 8 m/s. To make the wind conditions more realistic, turbulence intensity of 5% is added to the wind speed. The direction of wind flow is from west to east and hence the wind direction is considered to be at 0°. The wind turbine WT1 becomes the upstream turbine and WT2 becomes the downstream turbine. The turbine parameters and SOWFA parameters used for the simulation are tabulated in table 2-1.

Table 2-1: Turbine parameters for WT1 and WT2 used for simulation purpose

Parameters	**Values**
Domain size	2 km × 1 km × 0.65 km
Cell size	10 m × 10 m × 10 m
Time step	0.5 s
Rotor model	Rotating/generalized actuator disk model (ADM)
Turbine Model	NREL 5 MW
Rotor radius	63.2 m
Turbine spacing	5D
Ambient wind speed	8.0 m/s
Surface roughness	0.0002 m
Atmospheric stability	Neutral
Ambient turbulent intensity	5%
Fluid density (kg/m^3)	1.225
TSR limits [$\lambda_{lower} \lambda_{upper}$]	[12.0 13.0]

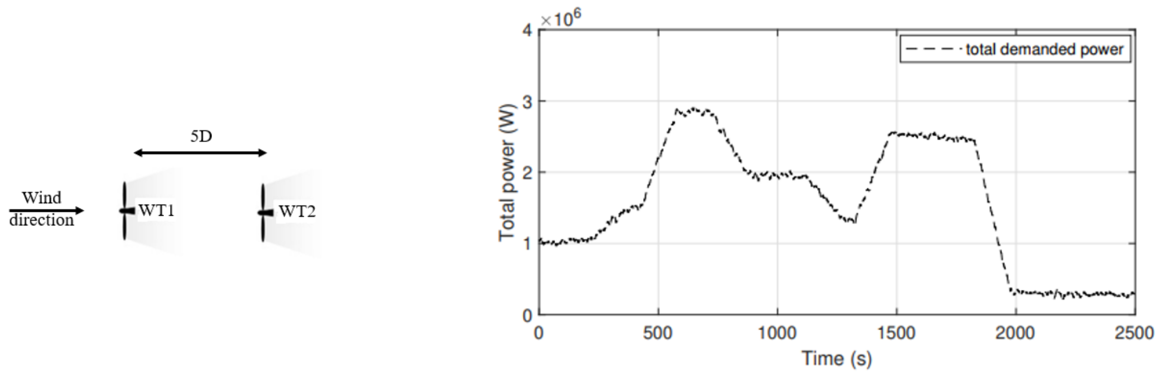

Figure 2-8: (a) Left: Layout of the two NREL 5 MW turbines placed at a distance of 5D. The turbines are considered to be oriented to the free-stream wind speed direction. **(b) Right:** Total power demand signal

Figure 2-8(b) shows the total power reference signal that needs to be tracked for a simulation time of 2500 seconds. The demand signal has been created with increasing and decreasing signals at different rates. Slight variations are also included over the entire power signal to make it more realistic. This total power reference signal is distributed among the turbines WT1 and WT2 such that, the WT1 turbine is demanded to generate 30% of the total demand and the down

2-4-2 Analysis

Figure 2-9 shows the dynamic simulation results for WT1 and Figure 2-10 shows the dynamic simulation results for WT2. For each of the turbines, there are 5 plots shown and it will be referred from (a) to (e) in top to bottom order for the discussion below.

- **(a):** The generated power from the turbine is plotted along with the turbine's power reference signal. The maximum power available is also plotted alongside. The maximum power that the turbine can generate for a estimated wind speed is calculated as $P_a = \frac{1}{2}\rho A C_p(\lambda_*, \beta_*)\nu^3$.

- **(b):** In this plot, the measured rotor speed of the turbine is shown. Minimum rotor speed required for stability represents the rotor speed corresponding to the optimal TSR value (λ_*) is calculated for the estimated wind speed. The rated rotor speed limits corresponding to the defined TSR limits (up-spin zone) are also plotted here.
- **(c):** This plot shows how the turbine's blades are pitched over the course of the simulation.
- **(d):** The generator torque commanded by the controller is shown in this plot.
- **(e):** Estimated wind speed obtained from the wind speed estimator is shown here.

Dynamic simulation results for WT1

With reference to Figure 2-9, WT1 is demanded to generate 30% of the total power reference signal. Once the power demand signal is received, the corresponding target C_p value to be tracked is determined. The power tracking law and the collective blade pitch controller operates together to increase the rotor speed and maintain it within the up-spin zone. This can be seen by increase in rotor speed and pitch angle in the initial few seconds from the start of simulation. The blade pitch controller remained active and hence the turbine's rotor speed was completely maintained within the up-spin zone throughout the simulation. The controller commands the torque based on the perfect tracking law. With sufficient wind speed available throughout the simulation, the WT1 was able to track the demanded power signal perfectly.

Dynamic simulation results for WT2

Figure 2-10 shows the dynamic simulation results for WT2. The wind turbine WT2 is the downstream turbine. The presence of WT1 before WT2 causes the formation of wakes. The presence of wakes makes the downstream turbine experience less wind speed and more turbulence. This is evident from the wind speed estimate plot where the estimated wind speed drops less than 7 m/s around 650 seconds in the simulation. The WT2 is demanded to track the 70% of the total power reference signal.

Once, the demand power signal is received for tracking, the turbine starts operating in the perfect tracking mode. As the power demand keeps rising and when the demand power is about to exceed the maximum power available corresponding to the estimated wind speed around 490 seconds, the measured rotor speed falls below the lower limit of the up-spin zone. The collective blade pitch angle drops to fine pitch angle leading to the increase in rotor speed. Additional generator torque based on the tracking law is applied. This leads to the decrease in the rotor speed. Meanwhile, the stored kinetic energy from the rotor is extracted to achieve perfect tracking. Once the rotor speed reaches the value equal to the minimum rotor speed required for stability, the turbine operates in the greedy mode and the controller commands a generator torque as per the greedy control law to regulate the rotor speed and operate the turbine at C_p^*. This phenomenon can be seen from 480 seconds to 700 seconds

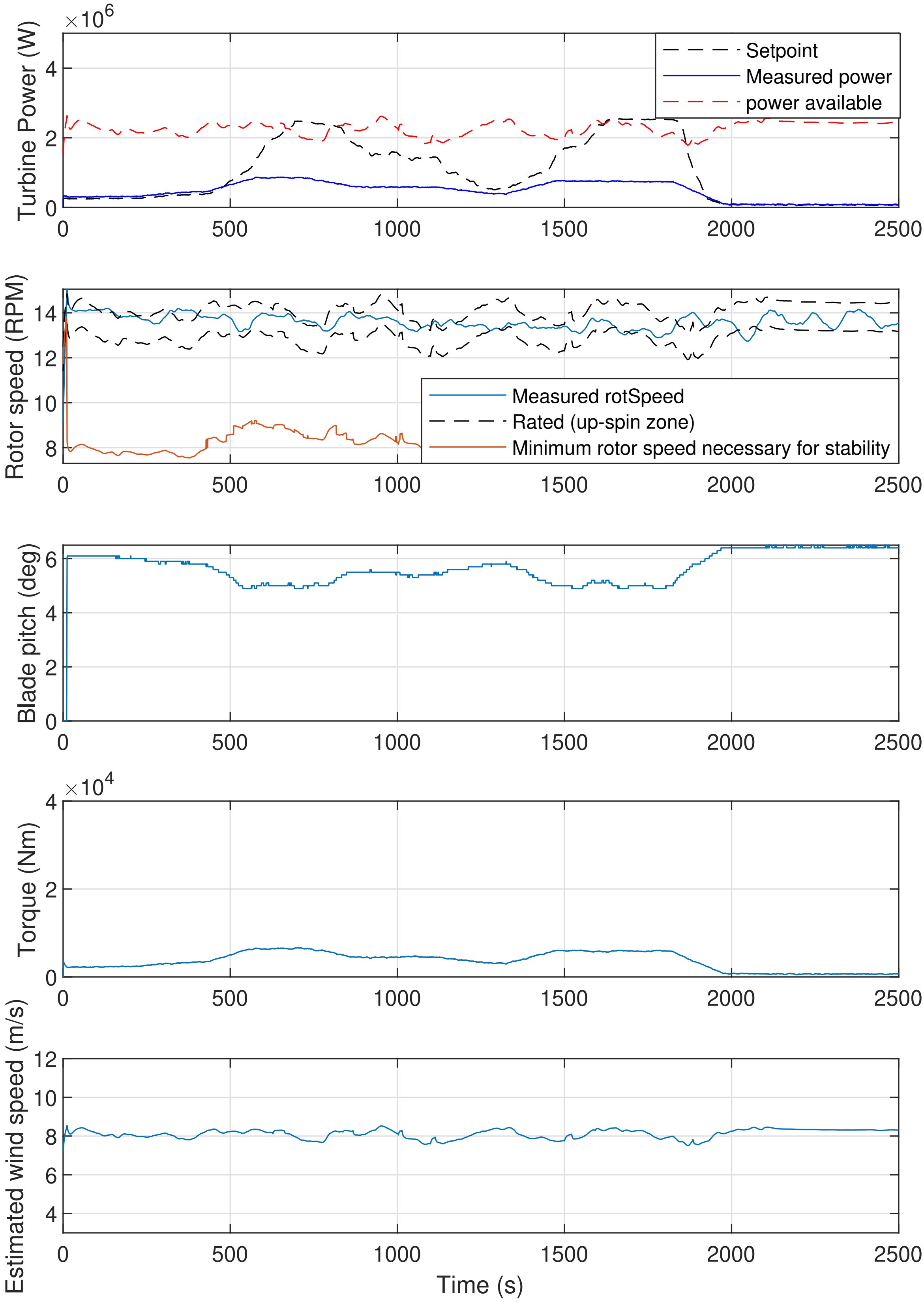

Figure 2-9: Simulation results for demanded power tracking (30% of total power demand) of the upstream turbine WT1 for 8 m/s wind speed with 5% turbulence intensity

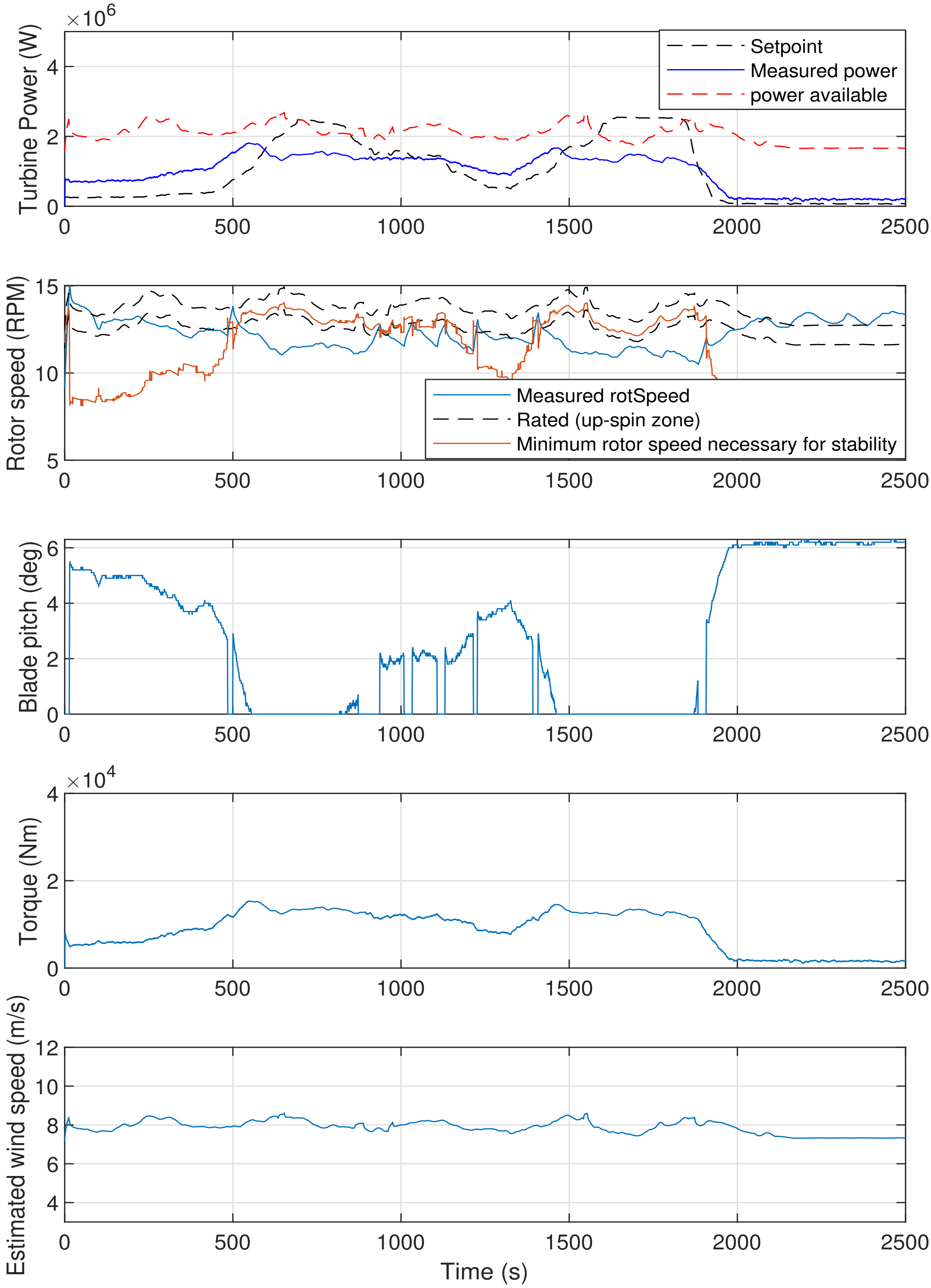

Figure 2-10: Simulation results for demanded power tracking (70% of total power demand) of the downstream turbine WT2 in the presence of wakes

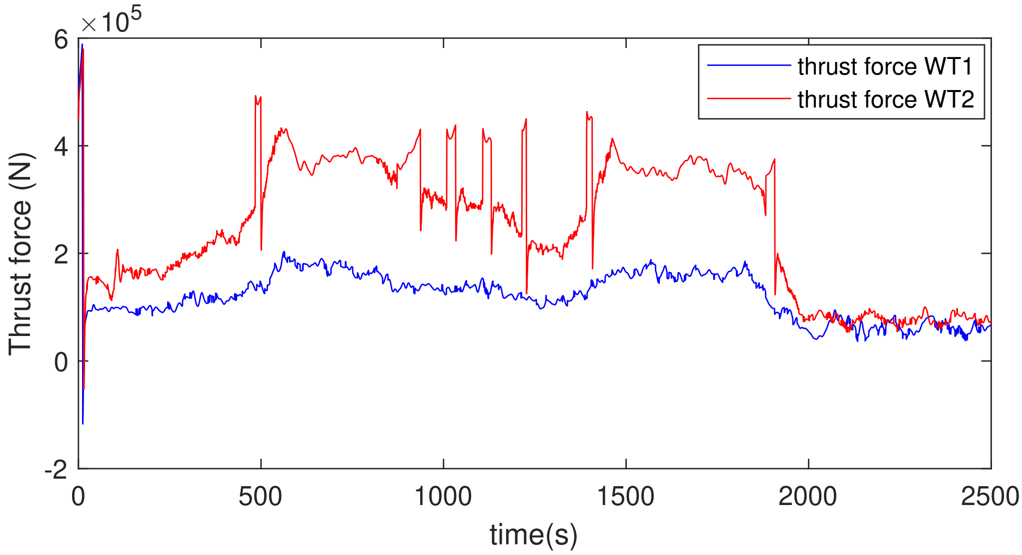

Figure 2-11: Comparison of the thrust force experienced by WT1 and WT2.

of simulation time where the turbine operates at C_p^* and generates power equal to maximum available power.

Once the demand becomes less than the available power, the controller again switches back to using the tracking law and collective blade pitch controller combination to track the power demand signal. The controller behaves the same, when the scenario of demand power exceeding available power happens between 1400 and 1900 seconds.

Thrust force comparison

The pitch angle variation in WT2 is more when compared to WT1. In WT1, the turbine completely operates in the perfect tracking mode throughout the simulation and hence blades of the turbine are always pitched between 5 and 7 degrees. But the turbine WT2 which is under the influence of wake turbulence, switches its mode of operation from perfect tracking to greedy/boosting mode. The pitch angle varies a lot throughout the simulation and the pitch angle falls frequently to the fine pitch value. The controller commands lower pitch angle compared to WT1 until 2000 seconds of simulation. As explained in [56], the thrust force experienced by the turbine reduces as the blades of the turbine are pitched more. This is evident from the comparison of the thrust forces experienced by WT1 and WT2 as shown in Figure 2-11.

Total power reference signal tracking

The ultimate aim is to track the total power reference signal shown in Figure 2-8(b). The summation of power generated from WT1 and WT2 is the total power generated and that is plotted and compared with the total demand power signal in Figure 2-12. The turbines together seems to track the demand curve very well apart from the regions where the demand exceeded the maximum available power as seen in the WT2 simulation plots.

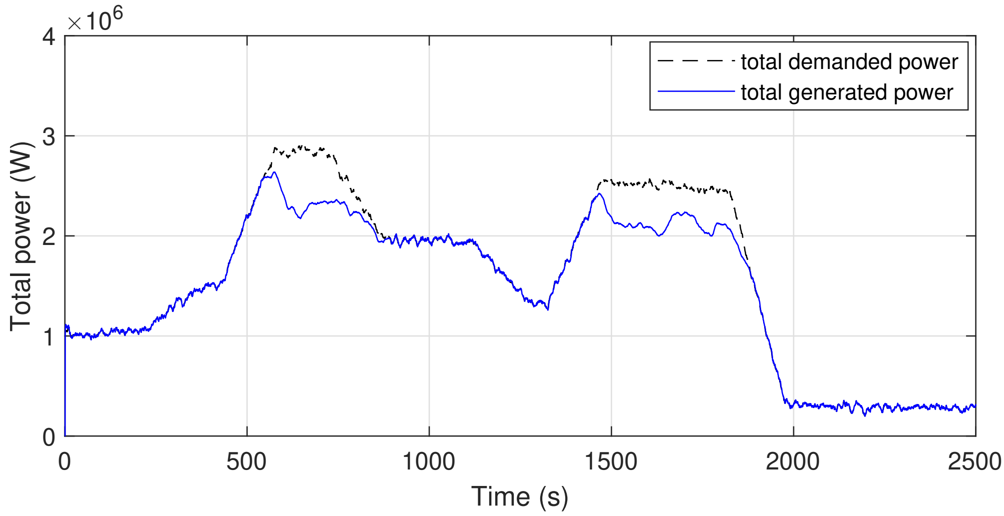

Figure 2-12: Total power reference tracking for WT1 and WT2.

With the objective to make the power produced from the entire wind farm track the overall power reference, it will be interesting to see how these individual turbine with power tracking feature perform in a wind farm in the presence of wake interactions. That will be discussed in the next chapter.

Chapter 3

Wind farm controller development

In Chapter 2, we saw about the development of a single wind turbine derating controller that enables the turbine to track a power reference signal. In this chapter, we will see about the development of the wind farm controller that coordinates all the turbines in the given wind farm and makes the total power generated out of the wind farm follow the overall power reference signal given to the wind farm. Section 3.1 discusses about the need for a closed loop wind farm controller with the help of a case study. The set point selection and distribution strategy will be discussed in Section 3.2. The development of closed loop feedback controller is discussed in the final section of this chapter.

3-1 Need for closed loop wind farm controller

In the previous chapter, a controller based on a tracking law for a single wind turbine was proposed and evaluated. The tracking controller makes the turbine to operate on tracking mode or greedy mode. In tracking mode, the controller makes the turbine generate power and perfectly track the reference power signal provided to the turbine. Whenever the demanded power exceeds the maximum available power (turbine operates at C_p^*), the controller makes the turbine operate in the greedy mode after extracting all the power from the stored rotor inertia. The performance of the proposed tracking controller was evaluated for a 2 turbine case where the upstream turbine was derated more than the downstream turbine. The upstream turbine tracked its reference signal perfectly, whereas, the downstream turbine which was under the influence of the wakes produced by the upstream turbine had to face low wind speeds for a brief moment. And in those moments of drop in wind speed, for an increasing power demand signal, the downstream turbine operated in greedy mode and produced the maximum power possible for that particular wind speed.

The next step is to evaluate the performance of the proposed controller for a large number of such wind turbines enabled with the power tracking capability. Consider a wind farm having 9 wind turbines arranged in the form of a 3×3 grid as shown in Figure 4-1 (refer chapter 4 for further explanation about the wind farm layout and simulation set up). Whenever there is an overall power reference command received from the TSO, a controller should distribute the overall reference signal as set points to all these 9 turbines. An open loop wind farm controller that only allocates and distribute the set points to individual turbines in an unwaked condition is employed. Let us consider that the simulations are made based on the scenario (refer scenario baseline explanation in chapter 4) where the each of the 3 rows of the wind farm is derated and commanded to produce 33.33% of the total reference signal.

Figure 3-1 shows the power generated from individual turbines of the farm where all the turbines are coordinated by an open loop wind farm controller that distributes set points to individual turbines based on the overall power reference signal. As seen from the figure, the wind farm controller has distributed the overall reference equally to all 9 turbines in the farm. The upstream turbines (turbine 1 , turbine 2 and turbine 3) are able to track their respective reference signal perfectly (as evidently seen from the exact overlap of the demand signal and the power generated). However, the downstream turbines, especially turbine 7, 8 and 9, which experienced the maximum turbulence due to the wakes and less wind speed went into greedy mode and generated the maximum possible power available at those moments.

When the power generated from all these 9 turbines are summed up and compared with the overall reference signal (as shown in Figure 3-2), we see that the wind farm could not track the reference properly after 500 seconds from the start of simulation. This is the moment where the downstream turbines went into greedy mode operation due to the influence of wake. The overall tracking error percentage also seem to be very high (> 20%). Also it can be observed from Figure 3-1 that even though the upstream turbines managed to perfectly track their respective reference signal, by being the upstream turbines, there is sufficient wind speed to generate even more power (as shown by the green line which indicates the maximum power available). This shows that the upstream turbine can be demanded to generate more power to compensate for the downstream turbine which are under the influence of wakes. Hence the wind farm controller should be developed in such a way that the set points to the individual turbines have to be redistributed considering the state of each turbine in the wind farm.

The same phenomenon has also been observed by Fleming et al. [21]. He observed that for the "high waking" case when an open loop wind farm controller performed poorly and the total power from the wind farm failed to track the reference. It has been concluded that a feedback controller is needed to solve this issue of set point distribution such that the set points can be appropriately adjusted to address the under performance that may be occurring at some turbines.

3-2 Set point selection and distribution

As stated in the previous section, if the total power output from a wind farm should follow a demanded reference trajectory, a wind farm controller needs to be there to coordinate the set points distributed to the individual turbines such that the power produced from each of the turbine sums up to desired amount. The coordination is made complicated when the turbines interact through wake losses. The turbines go into the greedy mode whenever there is increasing power demand and also the turbine is experiencing low wind speeds due to the wake.

Given the wind speed and direction, the wind farm controller's task is to distribute the set

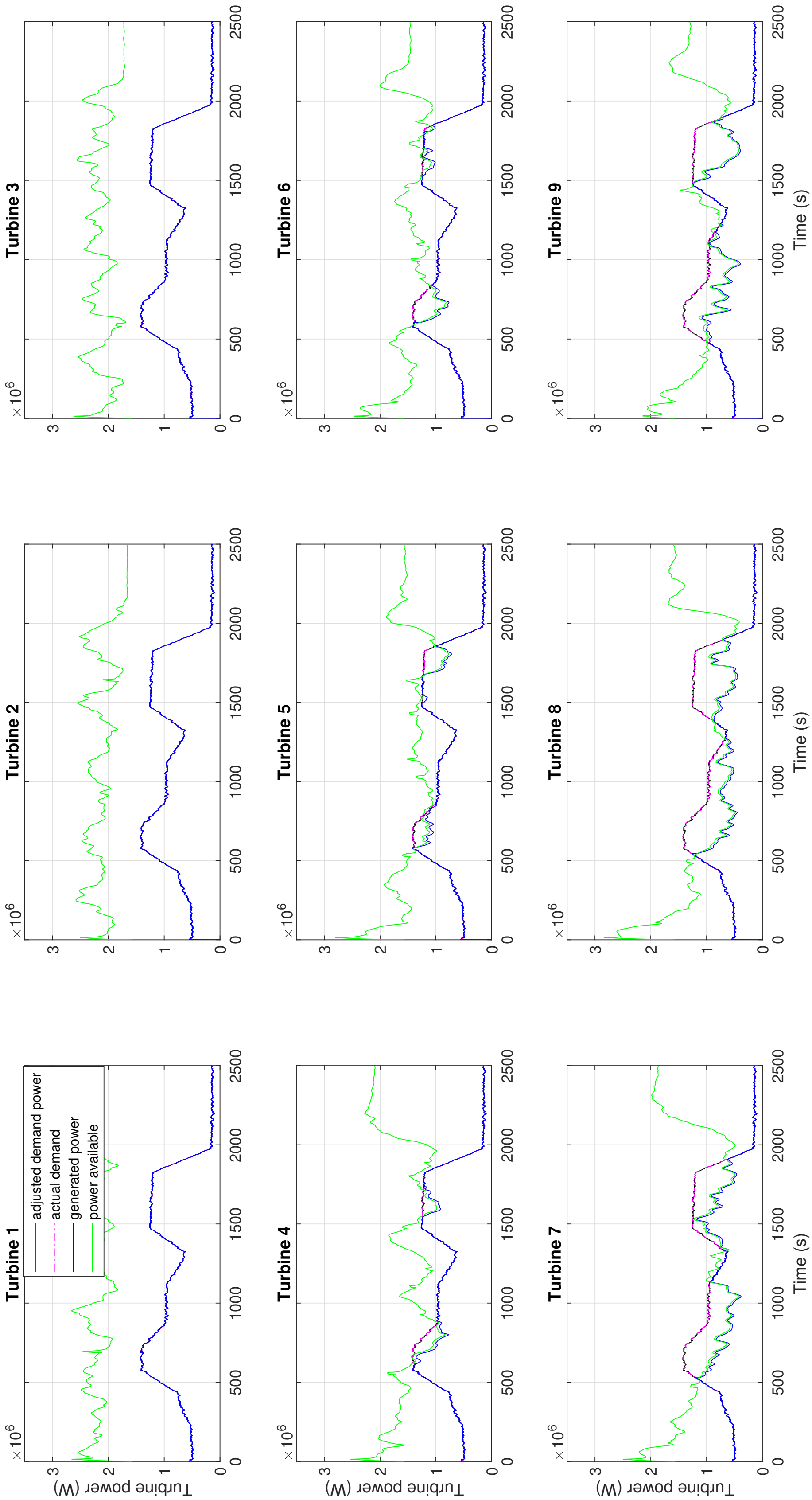

Figure 3-1: Individual wind turbine's power within the wind farm having a open loop wind farm controller. The reference signal is tracked for the case where all the turbine rows are equally derated.

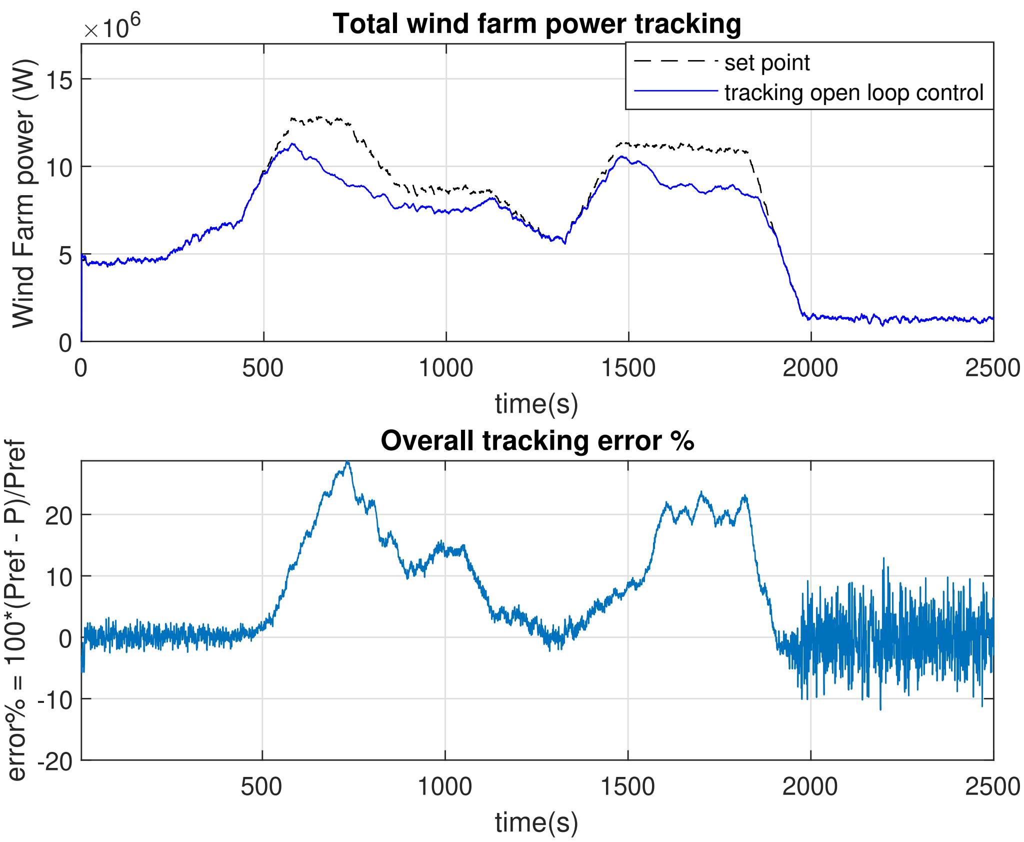

Figure 3-2: Top: Total power generated from the wind farm for the open loop wind farm control case compared with the overall power reference signal.
Bottom: Tracking error of the wind farm for the open loop wind farm control case.

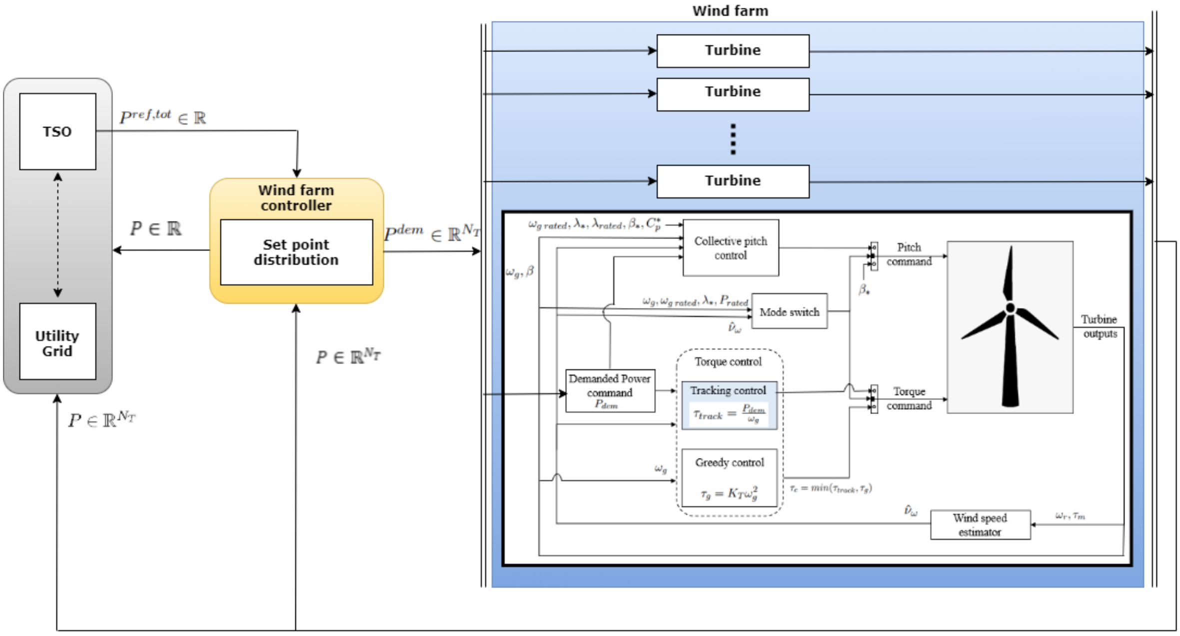

Figure 3-3: Schematic representation of APC for a wind farm where the individual turbines have their own controller to enable tracking of power reference signals. Based on the TSO command received and having the total power generated from the farm as the feedback, the wind farm controller re-distributes the set points to the individual turbines in the farm as set points based on whether the turbines in the farm are operating in tracking mode or greedy mode.

points over the N_T turbines as individual power demand set points, expressed as $P^{dem} \in \mathbb{R}^{N_T}$. Each turbine has its own power tracking controller that enables the turbine to track the respective power demand. The schematic of such a control system is shown in figure 3-3. Based on the availability of wind turbines and on the basis of wake interactions, the true optimal solution for set point distribution is a heterogeneous one. Based on different distribution of set points, the loads experienced by the turbines in the farm can also become significantly different. This again complicates the set point distribution.

3-3 Feedback control

As described in [21, 58], feedback control can be used to tackle the wind lulls that occur due to local turbulence. Hence, to improve the tracking performance of the wind farm, a simple feedback controller is proposed.

The notations and formulation of the concept are same as the one used in [58].

The wind farm has N_T number of turbines and all these turbines work together. The proposed control architecture is shown in Figure 3-4. The control signal that may increase the set points of the individual turbines is represented as $\triangle^{Pref} \in \mathbb{R}^{N_T}$.

The overall power generated out of the wind farm is representaed as $P^{tot} \in \mathbb{R}$. This overall power is the summation of the individual power generated from each turbine. Hence, $P^{tot} = \sum_{i=1}^{N_T} P_i$.

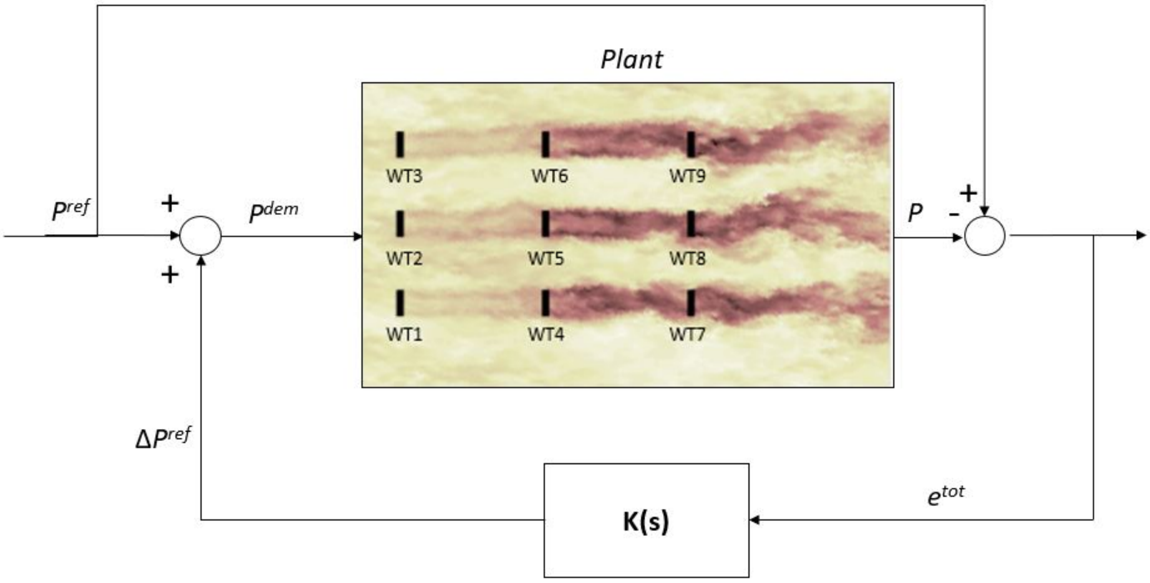

Figure 3-4: Schematic representation of the closed loop feedback wind farm control system (Adapted from [58])

Since the overall power reference is distributed as individual power reference to the turbines in the farm, this can be represented as, $P^{ref,tot} = \sum_{i=1}^{N_T} P_i^{ref}$.

The overall power $P^{tot} \in \mathbb{R}$ is defined as, and the overall power reference $P^{ref,tot} \in \mathbb{R}$ is defined represents the overal .

The total tracking error $e^{tot} = P^{ref,tot} - P^{tot} \in \mathbb{R} = \sum_{i=1}^{N_T} \left(P_i^{ref} - P_i\right)$. The overall tracking error is caused because of one or more turbines in the wind farm failing to follow ther respective power reference.

K(s) is the proposed controller. Whenever there is an overall tracking error only, this controller is active. The controller will distribute the overall tracking error among all the turbines.

3-3-1 PI controller

Before we get into the explanation of the closed loop controller development, on looking at Figure 3-5, we can observe that the total power signal tracks the overall reference signal with a delay of 0.5 s which is the sample time considered for the simulation. This means that the output tracks the input with a 0.5 s delay. On the assumption that when a turbine i in the farm is able to track the reference signal by a delay h, then the input output relation which is given by,

$$P_i(t) = P_i^{dem}(t - h) \tag{3-1}$$

Proprtional Integral (PI) controllers are the most common controllers developed for controlling a time delay system. The time delay model is approximated to frequency domain using Pade's approximation method and then the PI controller is developed over that model. The approach to develop such a stable controller for the considered time delay system can be referred

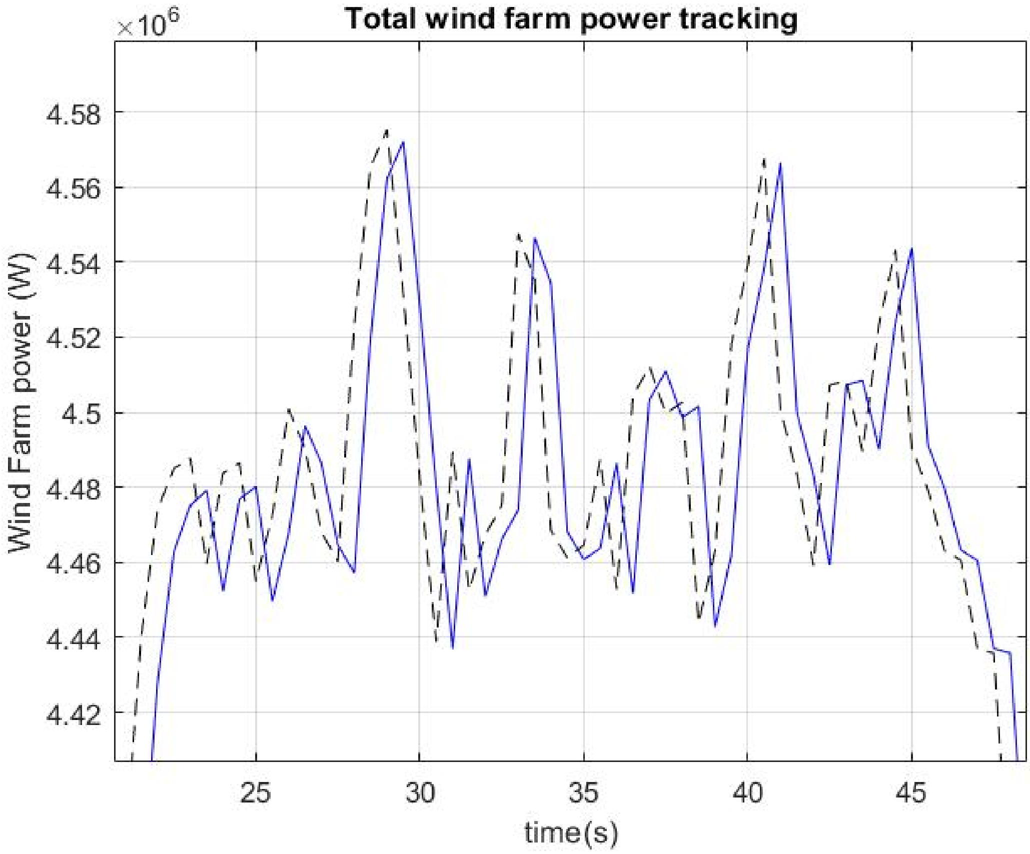

Figure 3-5: A zoomed up image of figure 3-2 total power generated from the wind farm for the open loop wind farm control case compared with the overall power reference signal

from [20, 45, 51] and the procedure/method to synthesize such a closed loop controller for a wind farm can be referred from [58].

Due to time constraints, the modelling of the time delay system and the synthesis of the PI controller is not done in this thesis and it is recommended for future works. The decision on controller gains for the PI controller has been made based on different simulation cases done for the controller gain values and that will be discussed in the next chapter.

Chapter 4

Simulations, results and discussions

In Chapter 3, we saw about the development of a closed wind farm controller that coordinates all the turbines in the wind farm and makes the total power generated out the wind farm follows the power demand reference signal. In this chapter, we evaluate that closed loop wind farm controller with respect to different simulation scenarios in a high fidelity simulation environment. The chapter is organized as follows. In Section 4.1, we see about the set up of the simulation environment, wind farm layout and then the scenario descriptions. Following that, in Section 4.2 the performance measures considered to evaluate the performance of the controller under different scenarios. The results of the simulations and the discussions related to the obtained simulation results are discussed in Section 4.3.

4-1 Simulation environment

The proposed closed loop wind farm controller for power tracking has been evaluated for a wind farm with 9 turbines using a high fidelity model. The model used is the Simulator fOr Wind Farm Applications (SOWFA) tool developed by the National Renewable Energy Laboratory (NREL). SOWFA is a open open source software package that is coupled with a framework which enables the users of SOWFA to investigate the effects of turbulence, weather patterns and terrains on the wind turbines and wind farms. It solves the 3D Navier stokes equation based on large eddy simulation methods. SOWFA has a super controller that allows the users to simulate coordinated multiturbine control of wind plants. Thereby, it allows the researchers to understand the performance of a wind farm better and enable them to improve on the performance and minimize the structural loads on turbine components. This high fidelity SOWFA model has high accuracy and hence the compromise is on the computational costs [2, 15].

4-1-1 Wind farm layout

The wind farm considered for the simulation consists of 9 NREL 5 MW reference turbines arranged in the form of 3×3 grid layout . The rotor radius of the turbine is 63.2 m (diameter

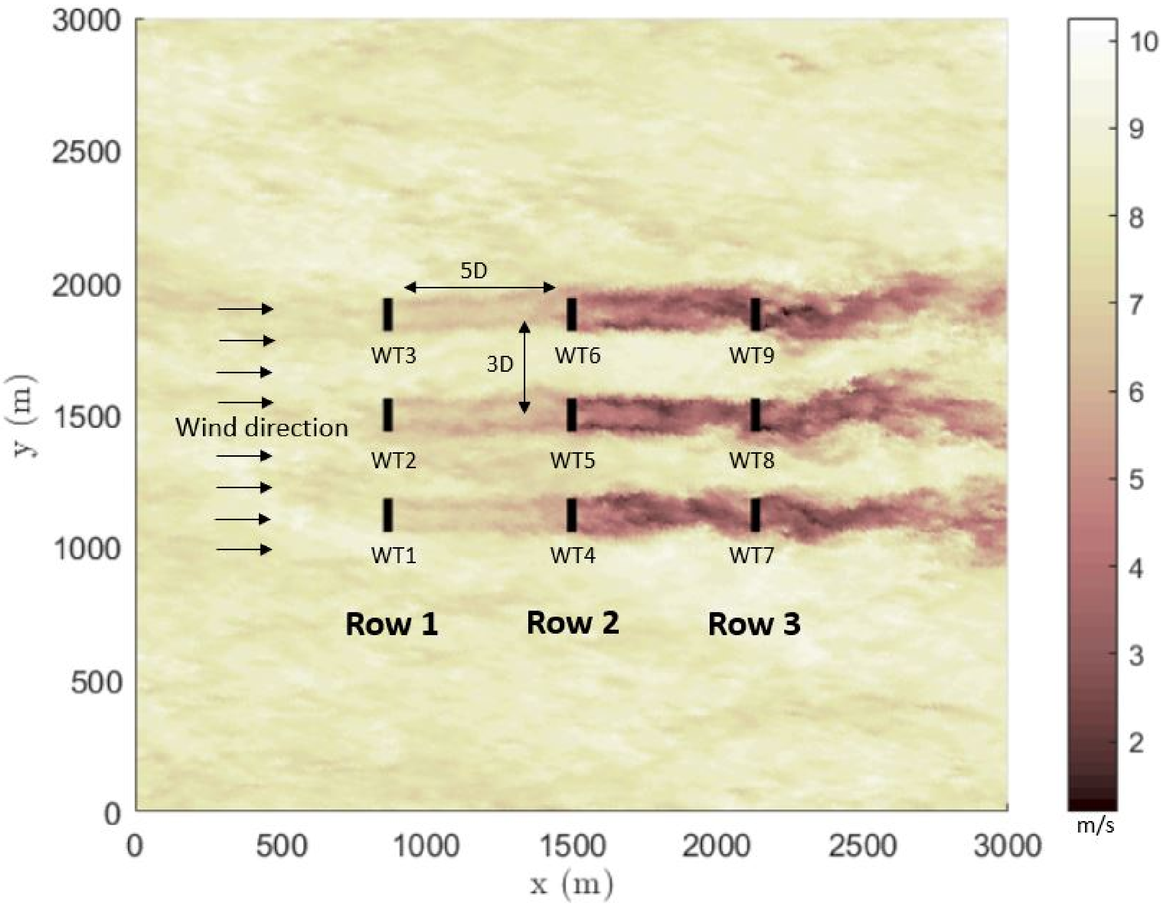

Figure 4-1: Layout of the simulated 3×3 wind farm. Background is an instantaneous horizontal slice of flow output taken from a SOWFA simulation. The wake formation and the corresponding wind velocity can be seen from the vertical bar on the right side of the figure. Turbine rows, spacing between the turbines and individual turbine reference names are also indicated

D = 126.4 m). The domain size is 3 km × 3 km × 1 km to allow for sufficient distance surrounding the turbines so that boundary effects negligible at the turbines. The turbines in the x-direction are spaced by 632 m (5D) and by 189.6 m (3D) in the y-directionas shown in figure 4-1. Table 4-1 specifies the SOWFA and turbine parameter values considered for setting up the simulation.

4-1-2 Scenarios for the simulation

If the wind farm is derated there are several ways to derate the individual turbines. In this section we will show 3 different derating scenarios.

van Wingerden et al. [58] and Fleming et al. [21], considered different set points the "high-waking" case. In those works, the overall power reference signal were distributed as set points over the different rows where the local reference signals are expressed in terms of the available power in the unwaked situation. Similarly, in this work, the overall reference signal will be distributed as set points to the different rows as indicated in figure 4-1. The individual

Table 4-1: 9 turbine wind farm simulation parameters

Parameters	Values
Domain size	3 km $\times$ 3 km $\times$ 1 km
Cell size	10 m $\times$ 10 m $\times$ 10 m
Time step	0.5 s
Rotor model	Rotating/generalized actuator disk model (ADM)
Turbine Model	NREL 5 MW
Rotor radius	63.2 m
Turbine spacing	5D $\times$ 3D
Ambient wind speed	8.0 m/s
Surface roughness	0.0002 m
Atmospheric stability	Neutral
Ambient turbulent intensity	5%

turbines in the farm has its own local feedback control (as explained in Chapter 2) that enables the turbine to track their respective reference signals. In this way, each of the turbine in a particular row of the wind farm, will have its own local reference signal expressed as some particular percentage of the overall reference signal in an unwaked condition. The turbines will be derated to that level and commanded to track that local reference signal.

Overall reference signal

The overall reference signal considered for all simulation scenarios is shown in Figure 4-2. This is the total power demand signal that needs to be tracked by the wind farm for a simulation time of 2500 seconds. The demand signal has been created with increasing and decreasing signals at different rates. Slight variations are also included over the entire power signal to make it more realistic.

Wind speed and direction

Simulations are performed with wind speed of 8 m/s. To make the wind conditions more realistic, turbulence intensity of 5% is added to the wind speed. The direction of wind flow is from west to east and hence the wind direction is considered to be at 0°. Hence the turbines of Row 1 in the wind farm layout, becomes the upstream turbines and the turbines in Row 2 and Row 3 are the downstream turbines which will be under the influence of wakes created by the turbines of Row 1 and Row 2 respectively.

Set point distribution scenarios

Given the wind speed and wind direction, as mentioned in the first paragraph of this section, the overall reference signal will be distributed as set points to the turbines corresponding to each of the row. Four different scenarios are considered for the simulations in this thesis.

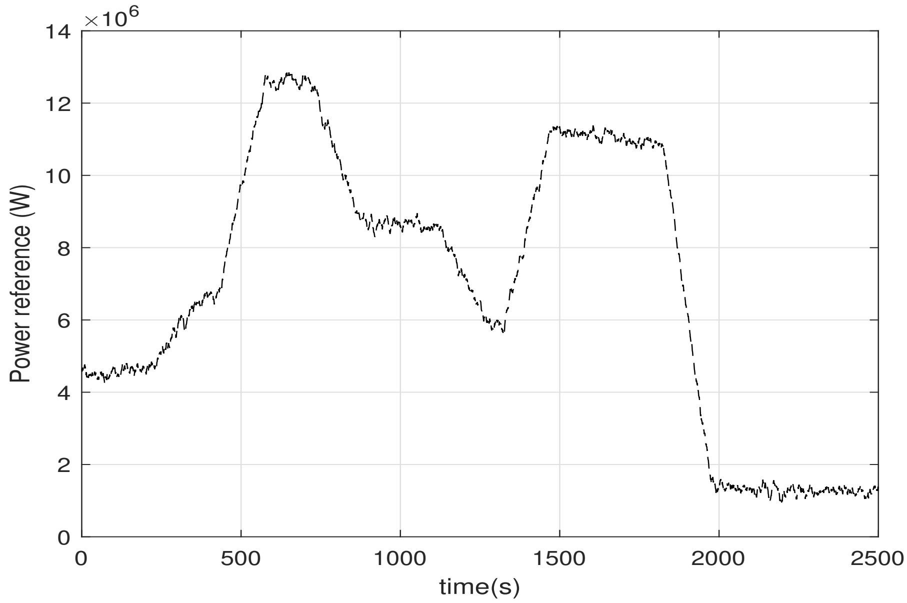

Figure 4-2: Reference power signal used for all the simulation scenarios

Scenario 1 (33-33-33): All the wind turbines in the farm have the same power command obtained by dividing the total reference into the number of turbines constituting the wind farm. In this way, each of the rows of the wind farm is derated to 33.33% of the overall power reference. Hence each individual turbine of Row 1, Row 2 and Row 3 will be derated and commanded to generated $\frac{1}{3} \times 33.33\%$ of the total power demanded.

Scenario 2 (16-33-49): The first row is derated to 16.83% of the overall power reference signal, the second row to 33.33% and the last row to 49.83%. In this way, the upstream turbines of Row 1 are more derated than the downstream turbine rows.

Scenario 3 (49-33-16): The first row is derated to 49.83% of the overall power reference signal, the second row to 33.33% and the last row to 16.83%. In this way, the downstream turbines of Row 3 are more derated than the upstream turbine rows.

Scenario baseline: In this scenario, the way in which the turbines in the wind farm are derated is similar to the one described in Scenario 1 (33-33-33). But in this Scenario baseline, the wind farm controller does not take the total power generated from the wind farm in its feedback. This means that in Scenario baseline, there is no feedback controller whereas the other scenarios mentioned above, the wind farm controller has the feedback loop. This scenario will be considered as the **baseline** and the other 3 scenarios will be compared with respect to this scenario.

4-1-3 Assessment criteria for controller performance

Since all the simulation results were derived from the same time domain, it is not suitable for directly comparing changes in power output with respect to different scenarios of distribution. To assess the performance of the 3 representative values are calculated for each of the simulation scenario and compared.

- To assess the tracking capabilities of the feedback controller, the **Root Mean Square (RMS) of the tracking error** is considered. The tracking error is given by the difference between overall power reference signal and teh sum of power generated from individual turbines.
- Another representative value err_p is also calculated to evaluate the power output generated from the wind farm. It is calculated as follows,

$$err_p = \frac{1}{T}\int_0^T \frac{\sum_{i=1}^{N} P_i(t) - P_{ref}(t)}{P_{ref}(t)} dt$$

  where N is the number of wind turbines in the wind farm, T is the total simulation time, $P_i(t)$ is the power generated by an individual turbine and $P_{ref}(t)$ is the overall power reference signal.

- The load experienced by the tower of the individual turbine is also calculated to assess the controller performance. To compare the tower load, the damage equivalence load (DEL) was used. The DEL for the tower load is calculated using the Palgrem Miner's rule [16] as,

$$DEL = \left(\frac{\sum_{k=1}^{n} n_k S_k^m}{N_{ref}} \right)^{\frac{1}{m}}$$

  Here m is a constant that is material dependent. It is related to the slope of the SN (stress to cycles to failure) curve for that particular material. For a steel tower, a value of 3.5 was used as the m value [33]. N_{ref} is a reference number that is equivalent to the equivalent number of cycles of DEL taken to become 1. It is commonly calculated from the simulation time. S_k is the stress experienced by the tower load. k represents the magnitude of the total tower load during a specified evaluation time. n_k is the number of occurrences (cycles) of S_k. Rainflow counting method is used to calculate the load cycles [8].

4-2 Results and discussion

In this section, before we see about the simulation results obtained for different scenarios on set point distribution, we will first see how the controller gain Ki of the PI controller is affecting the performance of the controller in achieving power tracking.

Table 4-2: RMS value of the tracking error comparison for different Ki values

Ki	RMS
$\frac{0.1}{9}$	516670
$\frac{0.3}{9}$	488920
$\frac{0.5}{9}$	478830
$\frac{0.8}{9}$	487450
$\frac{1.0}{9}$	487830
$\frac{2.0}{9}$	485810

Table 4-3: Mean DEL for tower load comparison for different Ki values

Ki	mean DEL
$\frac{0.1}{9}$	6.7824×10^7
$\frac{0.3}{9}$	6.6338×10^7
$\frac{0.5}{9}$	6.6145×10^7
$\frac{0.8}{9}$	6.6309×10^7

4-2-1 Effect of PI controller gain on the controller tracking response

We now have a PI based closed loop feedback wind farm controller. As mentioned previously in section 3-3-1, the synthesis of the controller has not been done in this thesis due to time constraints. To determine the gains of the PI controller, the overall tracking performance of the wind farm controller is evaluated for varying controller gains. The tracking performance is assessed based on the performance measures mentioned in the previous section. The controller gain that leads to better tracking performance was finalized to be the gain of the controller.

The simulations were set up based on the 'Scenario 1 (33-33-33)' where all the turbines in the farm are equally derated. Upon trial and error method it was realized that the Kp value of the PI controller affected the tracking performance always by introducing oscillatory behaviour. The controller performed well by having Kp as 0. Hence, for the rest of simulations the Kp value of the PI controller will be set to 0 and only the Ki value will be varied and the tracking performance will be evaluated for different cases. The simulations were made for the following increasing Ki values, Ki = $[\frac{0.1}{9}, \frac{0.3}{9}, \frac{0.5}{9}, \frac{0.8}{9}, \frac{1.0}{9}, \frac{2.0}{9}]$. Beyond that, the tracking performance was very unstable.

With reference to the Table 4-2, as the gains increased, the RMS value of the tracking error was found to decrease first and then increased again after $\frac{0.5}{9}$. This shows that having Ki value as $\frac{0.5}{9}$ produced the best tracking performance and beyond the performance declines for the other Ki values.

The mean of the DEL values for the case of the first 4 values were also calculated. The mean DEL values for the tower load for each of the case provide an insight about the average load experienced by the turbines in the wind farm for that particular case. Similarly from Table 4-3, we see that Ki value of $\frac{0.5}{9}$ produced the least mean DEL value for tower load. Hence the rest of the simulation values will use Ki value to be $\frac{0.5}{9}$.

Hence, the integral gain $\frac{0.5}{9}$, which produced the least RMS value and least mean DEL value was chosen and fixed as the Ki value for the rest of simulation cases.

4-2-2 Scenario baseline

For discussions regarding the simulations for this scenario, refer to Section 3-1 in Chapter 3.

4-2-3 Scenario 1 (33-33-33)

The results for this scenario are shown in Figures 4-3, 4-4. In Figure 4-3, the pink line represents the initial set point given to the turbines in the unwaked condition. The black line represents the new set points for each of the turbine where the initial set points are adjusetd by distributing the tracking error over all the turbines equally. The green line is the maximum possible power available that the turbine can generate when its operating at C_p^* for the instantaneous wind speed.

On looking at the individual turbine responses in Figure 4-3 and comparing it with the individual turbine responses with Scenario baseline as shown in Figure 3-1, we see that, in the case where there is feedback, the wind farm controller has evenly distributed the tracking error over all the turbines and increased the set points of all the turbines as well. The turbine in the upstream (turbine 1, 2 and 3) managed to generate more power and compensate for the unavailability of the downstream turbines.

The improvement in the overall tracking of the reference power signal can be seen clearly from the top figure in Figure 4-4. The presence of feedback controller ensured that the tracking performance is improved when compared to the case where there is no feedback controller. This is further justified by the reduced overall tracking error % value as seen from bottom figure.

4-2-4 Scenario 2 (16-33-49)

The individual turbines power tracking response with feedback control for the tracking of the reference signal based on this scenario can be seen in Figure 4-5. As seen from the figure, the initial set points for the downstream turbines are higher than the upstream turbines in the unwaked condition. As the downstream turbines are under the influence of wake turbulence, they are operating in the greedy control mode. The upstream turbine generates more power to compensate for the downstream turbines.

4-2-5 Scenario 3 (49-33-16)

The individual turbines power tracking response with feedback control for the tracking of the reference signal based on this scenario can be seen in Figure 4-6. Here the initial set points for the upstream turbines are higher than the downstream turbines in the unwaked condition. As the downstream turbines are under the influence of wake turbulence and hence operating in the greedy control mode, the upstream turbine generates more power to compensate for the downstream turbines.

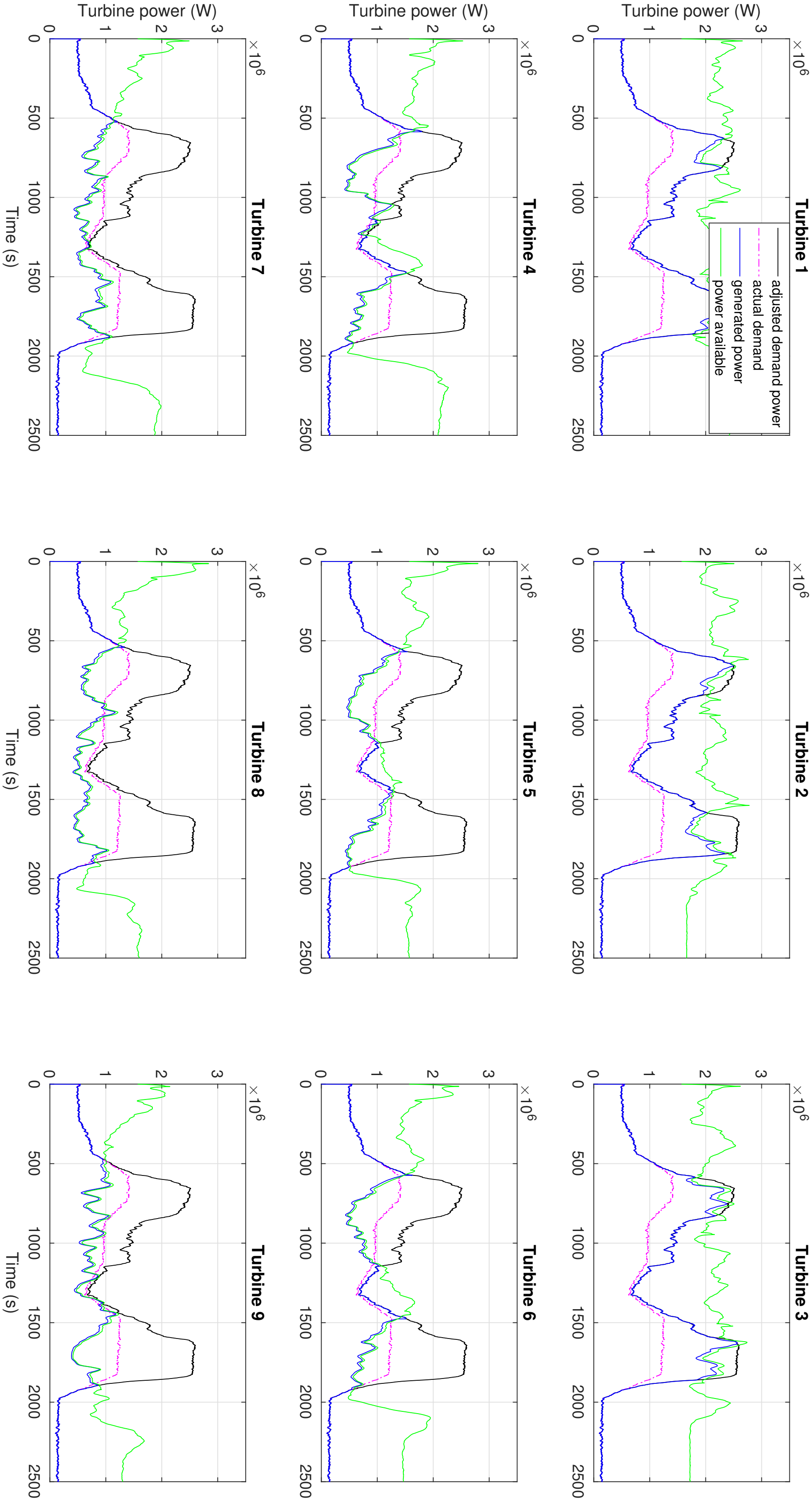

Figure 4-3: Individual wind turbine power where we track the power reference signal for Scenario 1 (33-33-33).

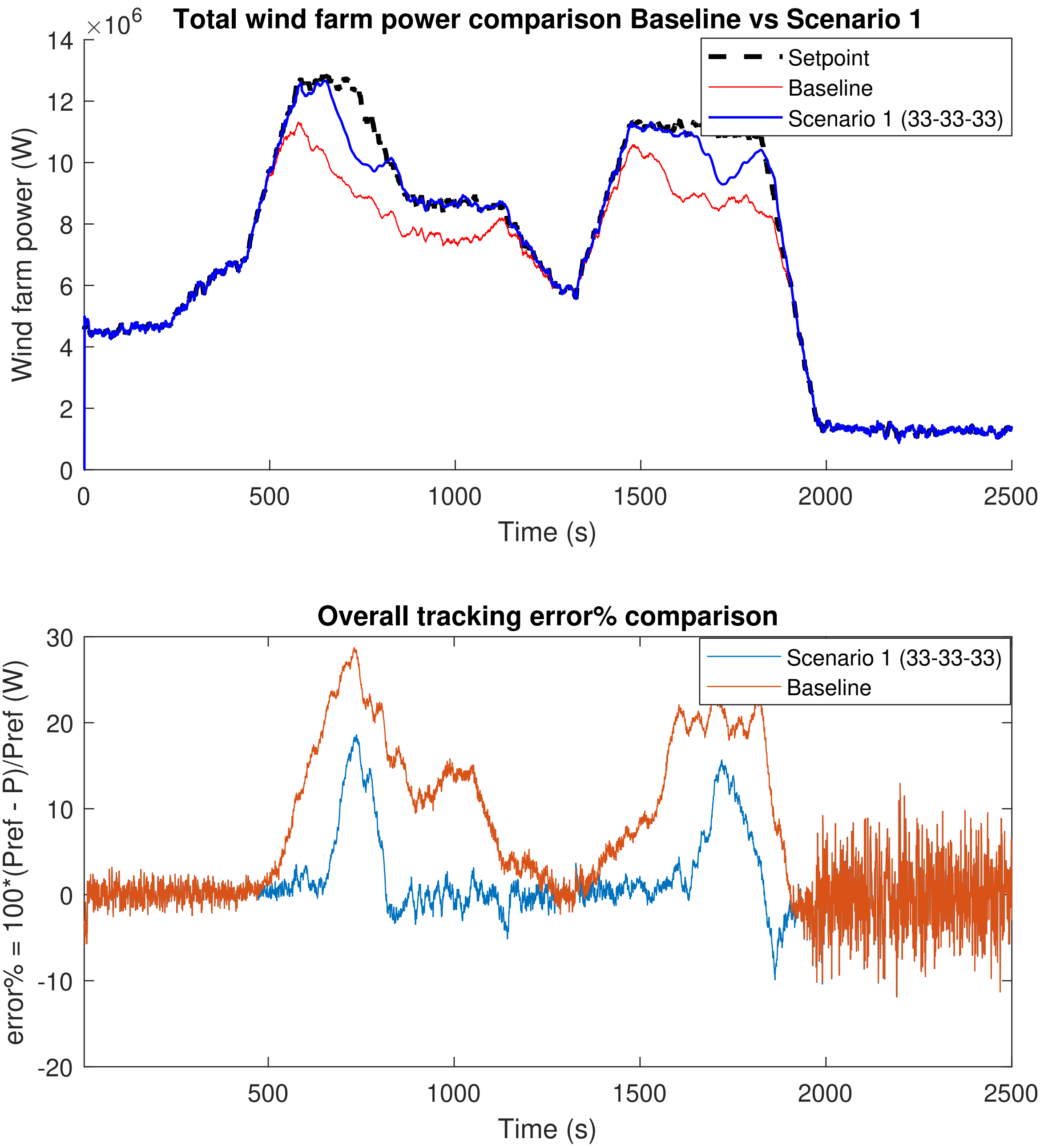

Figure 4-4: Top: Total power wind farm power comparison-Baseline vs Scenario 1. Bottom: Overall tracking error % of the wind farm comparison-Baseline vs Scenario 1.

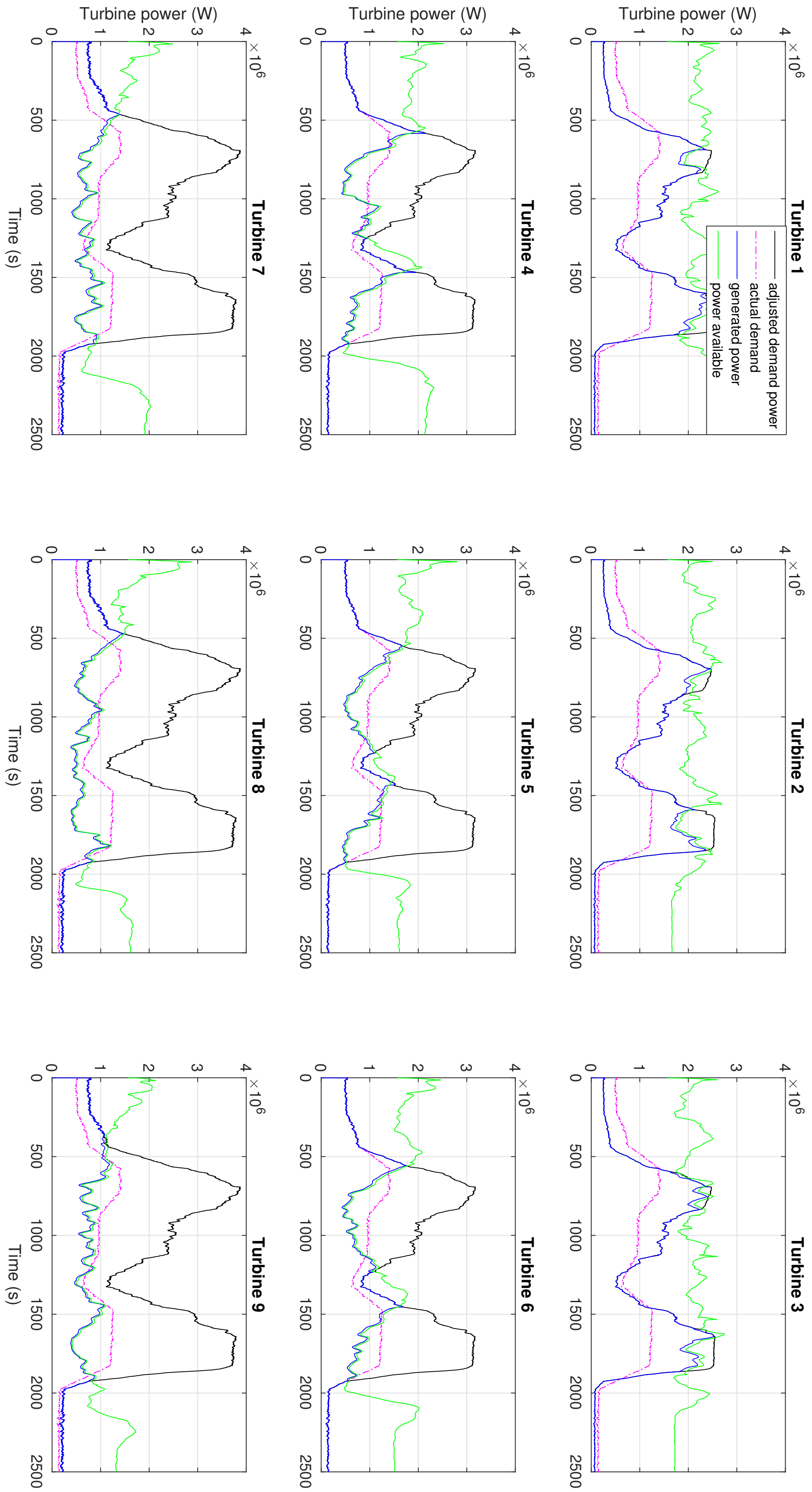

Figure 4-5: Individual wind turbine power where we track the power reference signal for Scenario 2 (16-33-49).

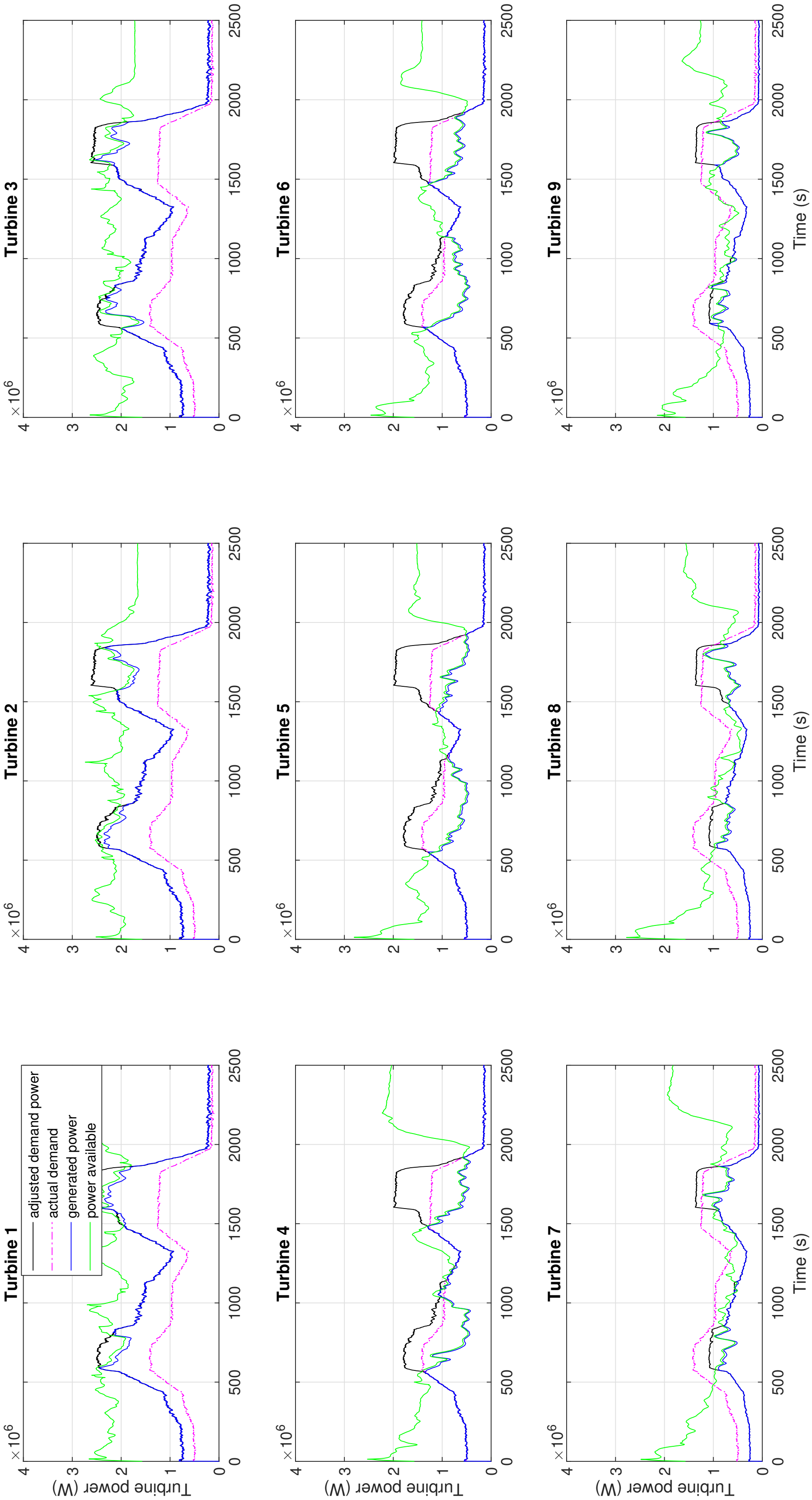

Figure 4-6: Individual wind turbine power where we track the power reference signal for Scenario 3 (49-33-16).

Table 4-4: Comparison of 4 scenarios based on performance scores

Scenario	err_p	RMS
Scenario Baseline	340.8980	1205000
Scenario 1 (33-33-33)	63.7576	490130
Scenario 2 (16-33-49)	52.5537	443540
Scenario 3 (49-33-16)	81.2700	553540

4-3 Comparison of results for different scenarios

The total power generated from the wind farm from all the 4 scenarios of simulation are plotted and shown in Figure 4-7 and a comparison plot is shown in Figure 4-8. The bottom plot in Figure 4-8 shows the comparison of the maximum available power in the wind farm for each of the simulated scenario. Visually, on observing the plots, the scenario 2 (16-33-49) where the upstream turbines of row 1 are derated more than the downstream ones performed better than the other three scenarios. Derating the upstream turbines more ensures that the wakes experienced by the downstream are less and hence the downstream turbines face more wind velocity. With higher wind speeds available, there is always scope for the turbines to generate more power. This can be seen from the bottom plot of Figure 4-8 where higher available power is there for scenario 2 compared to the other scenarios. The performance scores are tabulated in Table 4-4. The scores also indicate the same that Scenario 2 has the least RMS value of tracking error and least tracking error percentage value when compared to the other 3 scenarios.

The loading on the structural components of the individual wind turbine is a very important aspect considered by the wind farm operators and stake holders. SOWFA allows us to calculate the loads experienced by the tower base of the individual turbines. The damage equivalent loads for the tower base moments are calculated for the different scenarios and presented in figure 4-9. The DEL values are normalized with respect to the DEL value of turbine 1 in the Scenario baseline. On comparing the normalized DEL's for different scenarios, the loads are better distributed over the windfarm in Scenario 1 (33-33-33) where the normalized DEL value ranges between 0.9 and 1.1 for all the 9 turbines. In scenario 2 (16-33-49), the upstream turbines and turbine 4 experience less load when compared to the other turbines downstream. Conversely, in scenario 3 (49-33-16), the upstream turbines experience more loading than the downstream turbines. The turbine 9 in scenario 2 experience the least load in that scenario. The reason for it to experience the less load can be justified by looking at the instantaneous horizontal slice of flow output taken from SOWFA for scenario 2 as shown in Figure 4-10 and also the thrust forces comaprison in Figure 4-11. The turbine 9 experience the lowest wind speed compared to other turbines due to the wake effect. Since thrust force is a funtion of square of wind speed, the reason for experiencing such low loads can be justified.

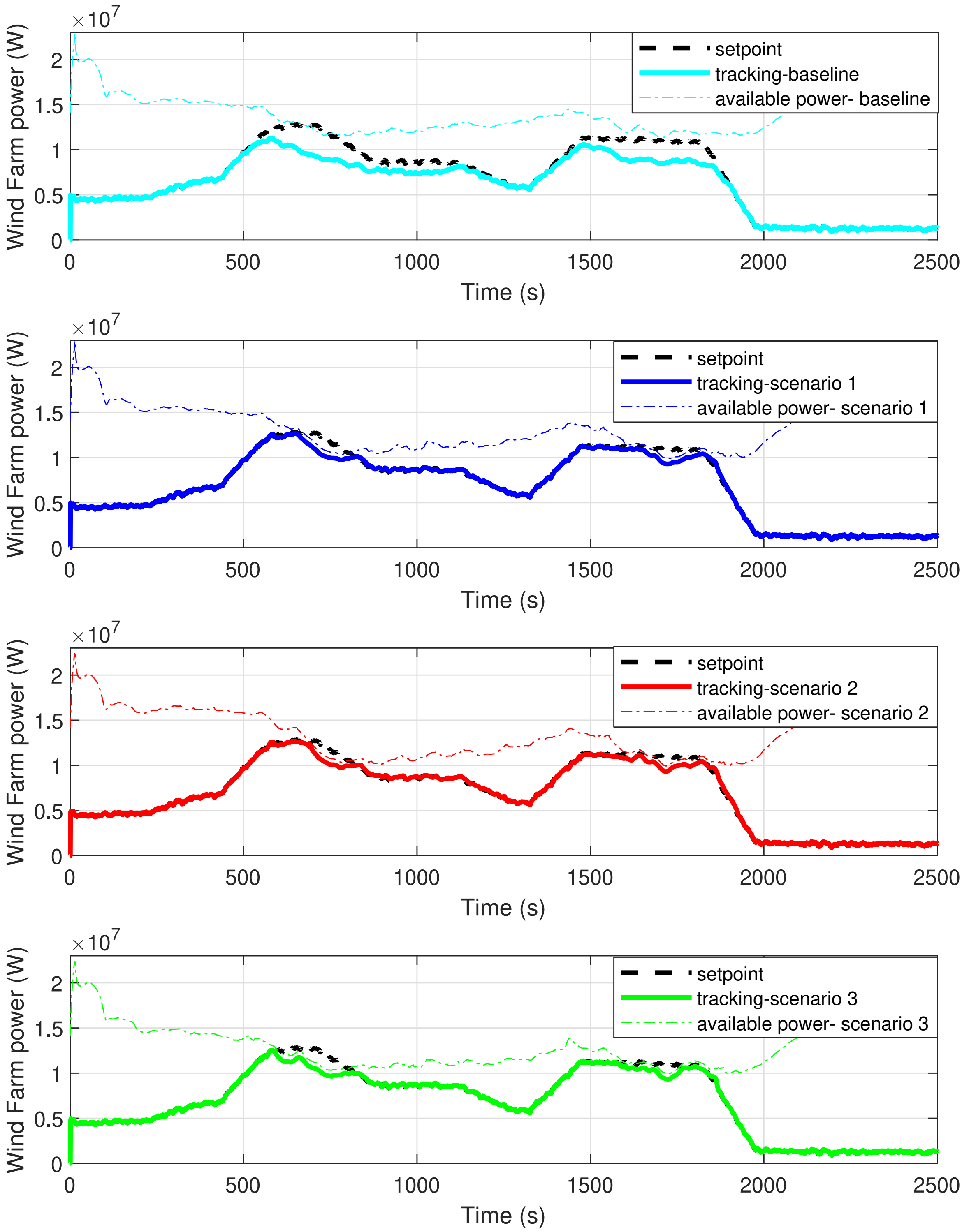

Figure 4-7: Total power of the wind farm with feedback control simulated for all 4 set point distribution scenarios.

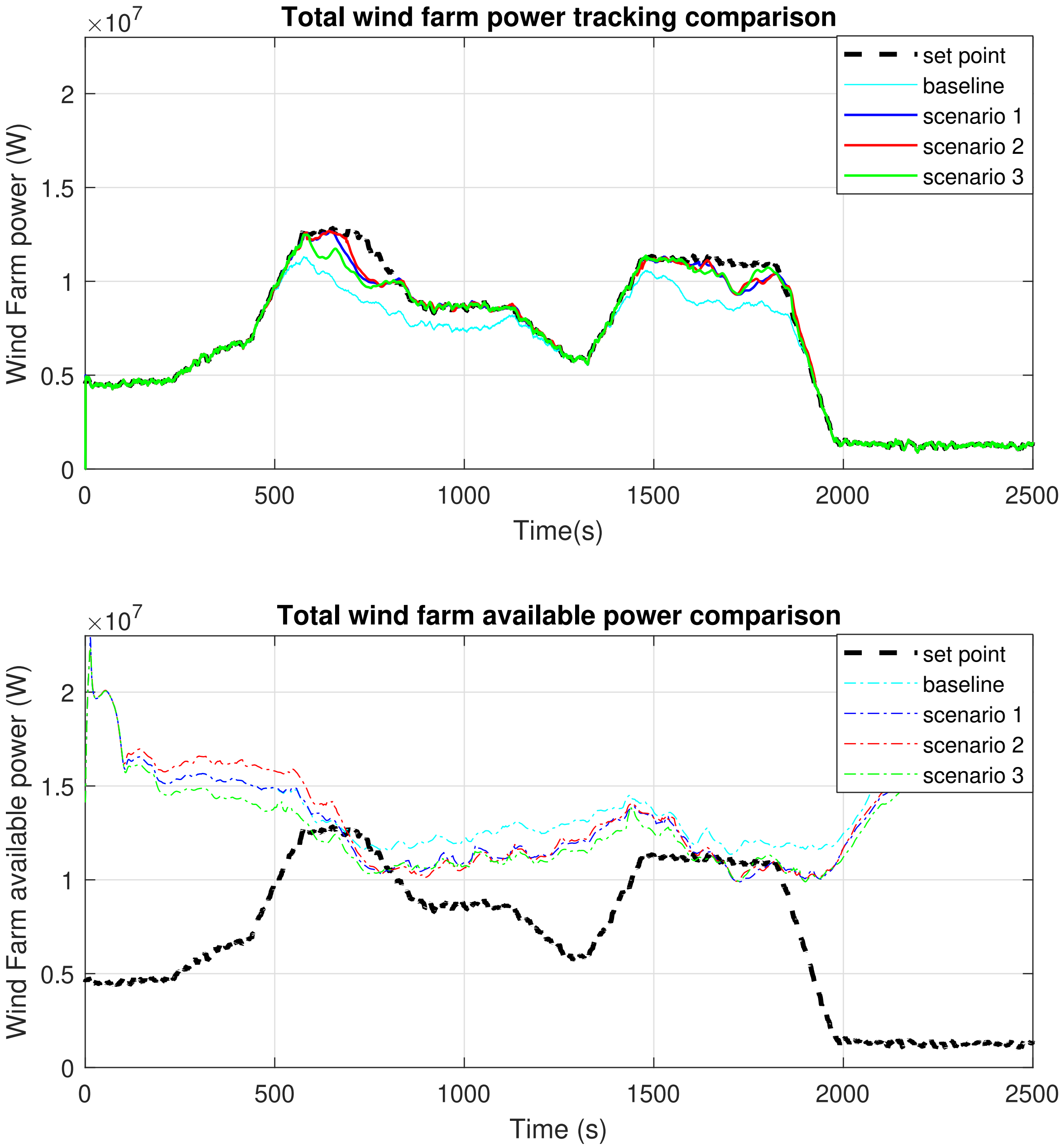

Figure 4-8: Top:Comparison of total power of the wind farm simulated for all 4 set point distribution scenarios.
Bottom:Comparison of available power of the wind farm simulated for all 4 set point distribution scenarios.

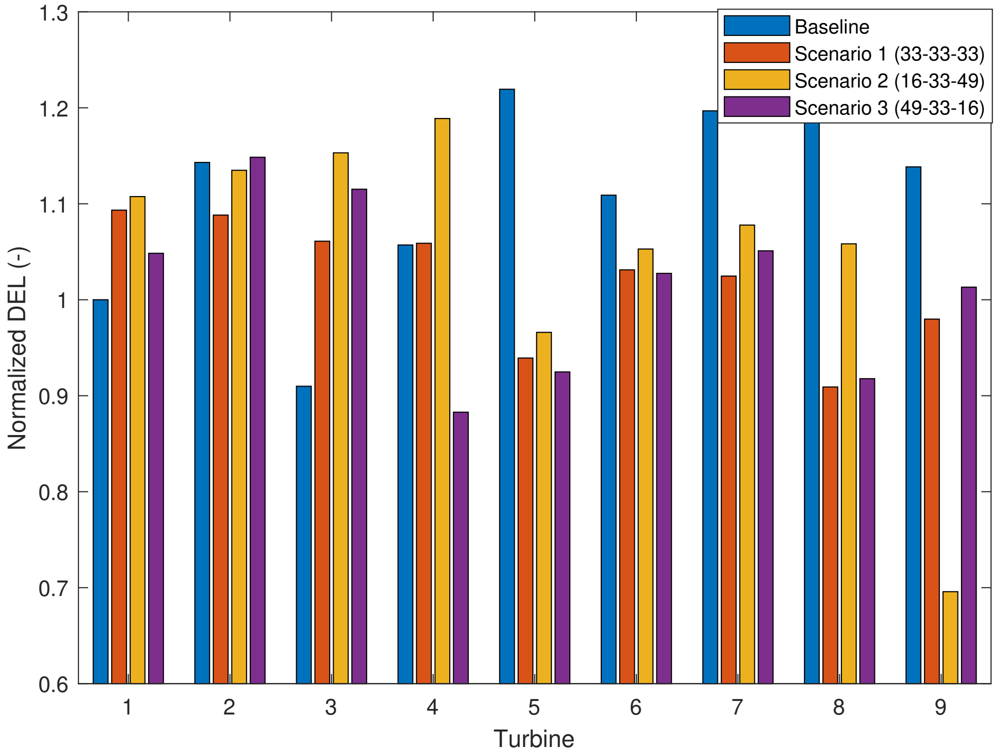

Figure 4-9: Damage equivalent loads for the tower base moments normalized with respect to turbine 1 operated in Scenario baseline.

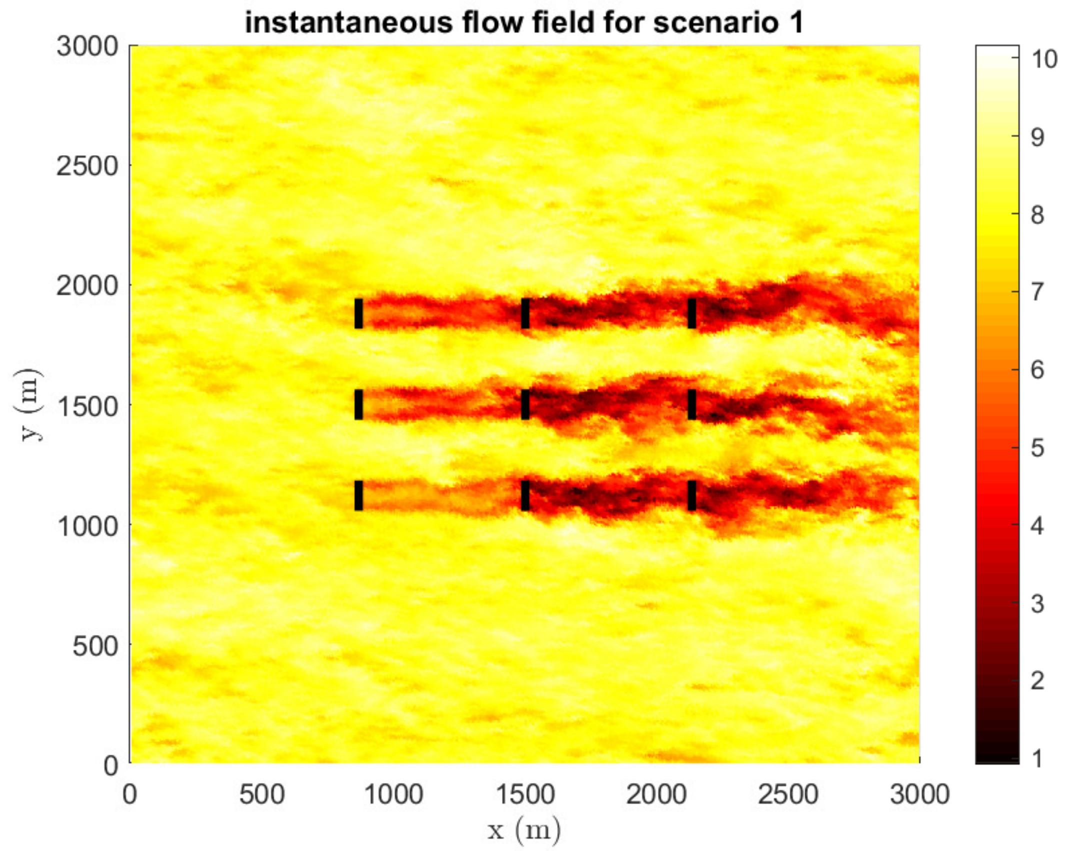

Figure 4-10: instantaneous horizontal slice of flow output taken from SOWFA for scenario 1

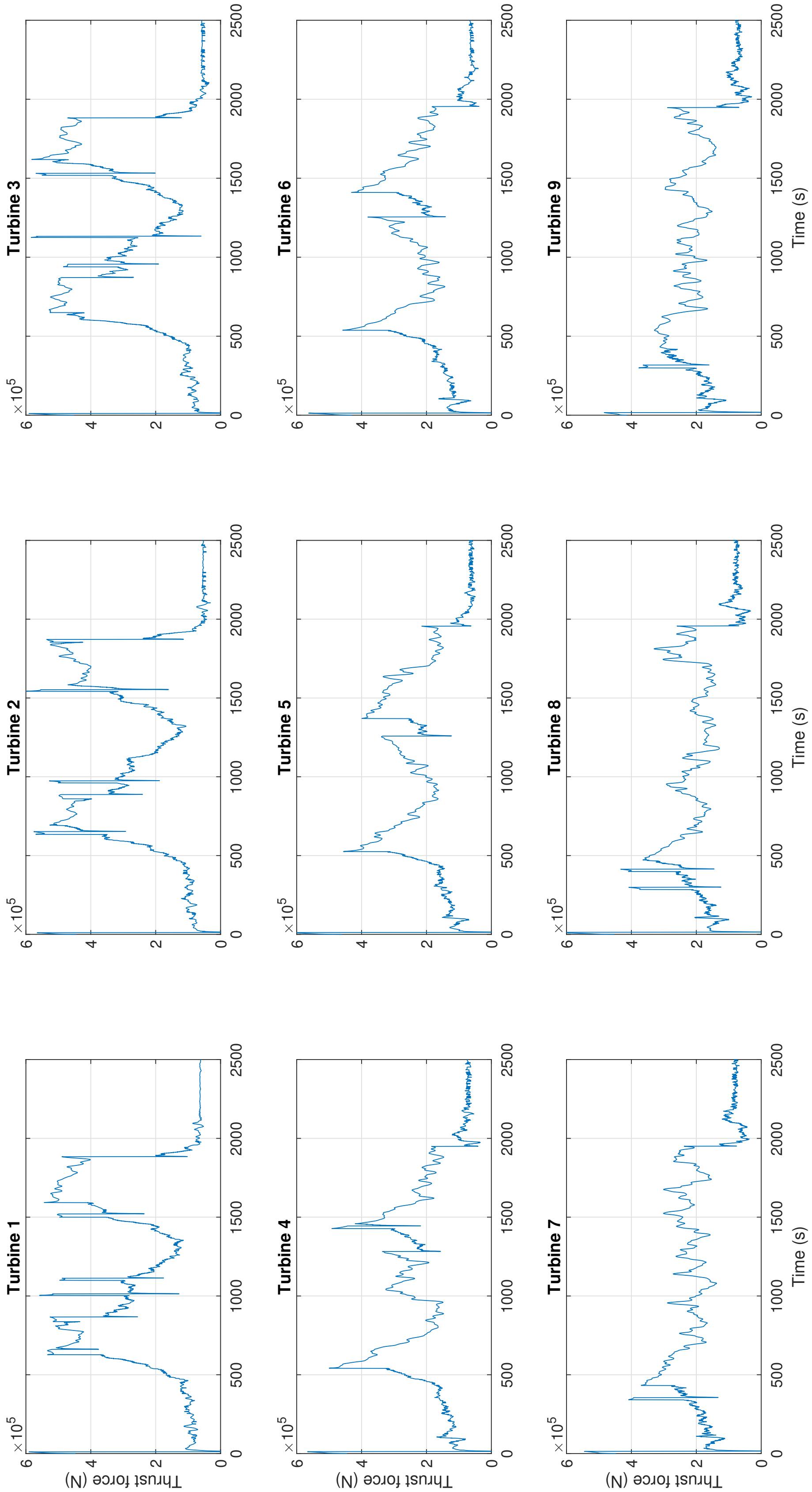

Figure 4-11: Thrust force of individual turbines in Scenario 2.

Chapter 5

Conclusions and recommendations

The objective of this thesis is to develop a wind farm controller to provide APC for the wind farm and then evaluate the performance of the proposed controller under different set point distribution scenarios. With this goal in hand, the thesis was framed to answer a set of problem statement questions as mentioned in section 1-3 of the introduction chapter. The conclusions of this thesis will be presented here by answering to those problem statement questions. Recommendations for future works have also been presented in the end.

5-1 Conclusions

- ***Can a wind farm controller be developed to provide APC for waked wind farms, where, the set point selection and distribution happen without estimating the available power at each turbine?***
  Yes. Considering that the estimation of available power at every time step is a challenging problem, a closed loop wind farm controller has been developed in such a way that it eliminates the dependence on the estimation of available power. As a first step to achieve this, a single wind turbine tracking control law was developed to enable the turbine to track its local power set points. This turbine level control system consists of a wind speed estimator which estimates wind speed. With the estimated wind speed alone, the tracking law was developed such that, based on the wind speed, it can command the turbine to operate in the perfect tracking mode or on a greedy control mode. Having eliminated the dependence of the estimation of available power even at the turbine level, a closed loop wind farm controller was developed as the next step. This closed loop wind farm controller takes the total power generated out of the wind farm as the feedback signal and based on the availability of the turbines (greedy or tracking mode), the controller distributes the overall tracking error + reference signal to the individual turbine. Thereby, the turbines other than those operating in the greedy mode, compensate and generate extra power to make the total power generated out of the wind farm to track the overall reference signal.

- ***How is the tracking performance affected when the gains of the wind farm controller are changed?***
  The integral gain Ki was the tuning parameter for the closed loop wind farm controller. As the synthesis of the closed loop wind farm controller was not done in this thesis, in order to determine the gains of the PI controller, the overall tracking performance of the wind farm controller was evaluated for varying controller gain values, and the controller gain that lead to better tracking performance was finalized to be the gain of the controller. Based on this idea, the simulations were performed for different Ki values. As the gains increased, the RMS value of the tracking error was found to decrease first and then increased again after $\frac{0.5}{9}$. This shows that having Ki value as $\frac{0.5}{9}$ produced the best tracking performance and beyond that, the performance declines for the other Ki values. The same pattern can also be observed in the mean DEL values and the Ki value of $\frac{0.5}{9}$ had the least value of mean DEL. Thus, $\mathrm{Ki} = \frac{0.5}{9}$ produced least RMS value and least mean DEL value and hence was chosen and fixed as the Ki value for the rest of simulation cases. This trial and error method of finding the right parameter value for the controller gain might not work in all cases. Synthesis of the controller needs to be done considering the stability conditions.

- ***How do different set point distributions affect the tracking performance of the controller and how does the load experienced by the turbines differ based on different set point distribution scenarios?***
  Derating the upstream turbines more ensures that the wakes experienced by the downstream are less and hence the downstream turbines face more wind velocity. With higher wind speeds available, there is always scope for the turbines to generate more power. On comparing the DEL's for different scenarios, the loads are better distributed over the turbines of the windfarm in scenario 1 (33-33-33). The turbines in the baseline scenario faced the highest loads among all 4 scenarios. In scenario 2 (16-33-49), the upstream turbines and turbine 4 experience less load when compared to the other turbines downstream. Conversely, in scenario 2 (49-33-16), the upstream turbines experience more loading than the downstream turbines. Different scenarios produced different loading patters. On observing the loading patterns, the presence of feedback loop on the wind farm controller not only improved the tracking performance but also it reduced the loads experienced by the individual turbines.

Concluding points

- Closed loop wind farm controller is necessary to obtain better tracking performance and reduced structural loading on the turbines of the wind farm.

- When upstream turbines are derated more than the downstream turbines, the tracking performance improved because the downstream turbines were able to experience more wind speed.

- Different set point distribution scenarios resulted in different loading patterns. It is upto the wind farm operator and the stake holder to decide which type of loading pattern would they prefer.

5-2 Recommendations

- **More scenarios for simulation:** Looking at the results obtained in chapter 4, we can see that the performance of the proposed controller was affected by different set point distribution scenarios. But all the simulation scenarios were tested for a fixed wind speed and direction. It will be interesting to observe how the controller performs for varying wind speeds and also with changing directions.

- **Optimization procedure for distribution of set points based on load** For each of the scenario simulated in this thesis, the initial set points to the individual turbines was allocated row wise by the wind farm controller. Based on the availability of the individual turbines and to compensate for the wake losses, the wind farm controller redistributed the set points such that the available turbines can compensate for the those turbines which are unavailable for power tracking. We also saw that different different scenario produced different loading patterns. If the load experienced by the individual turbines have to be reduced and maintained below a certain level, then a separate optimization procedure needs to be developed for redistributing power set points having loads of the turbines as constraints.

- **Power reserve maximization strategy:** In this thesis, the objective was just to track the power demand requirements obtained from the TSO. Another method of APC demands to maintain a certain amount of reserve power throughout the wind farm as this reserve power can be used for providing primary or secondary frequency responses. When certain amount of reserve has to maintained throught the wind farm, the individual turbines have to be operated in such a way that a certain power is reserved at each individual turbine in the farm. To achieve this, the set point redistribution needs to be done with the objective of maximizing the power reserve.

- **Adaptability of the control algorithm for turbines with different power generation capacity:** The single wind turbine tracking control algorithm is developed for a NREL 5MW turbine. If the algorithm has to implemented on a 10 MW wind turbine or a 2 MW turbine, it will be interesting to see how the control algorithm needs to be adapted to suit that turbine. Also, the C_p and C_T curves derived for NREL 5MW turbine through SOWFA simulation model differs slightly from the actual NREL 5MW specifications. If the algorithms have to implemented and real time testing have to be done, it will be interesting to see how much the algorithm needs to be adapted.

- **Wind farm controller synthesis:** The synthesis of the closed loop wind farm controller based on Pade's approximation techniques was not done in this thesis due to time constraints. So that needs to be done to analyse the stability factors of the controller and its tuning parameters.

- **Stability proof for I&I estimator:** As mentioned in Chapter 2, the stability of the estimator needs to be proved mathematically when collective pitch angle β parameter has been included into the estimator design.

Bibliography

[1] Global wind installations. https://library.wwindea.org/global-statistics-2018-preliminary/, Accessed: 2019-09-17.

[2] Sowfa. https://www.nrel.gov/docs/fy15osti/63378.pdf, Accessed: 2020-06-27.

[3] Wind power capacity worldwide reaches 597 GW, 50,1 GW added in 2018. https://wwindea.org/blog/2019/02/25/wind-power-capacity-worldwide-reaches-600-gw-539-gw-added-in-2018/, Accessed: 2019-09-17.

[4] Wind turbine aerodynamics. https://en.wikipedia.org/wiki/Wind-turbine_aerodynamics#Thrust_coefficient, Accessed: 2020-06-27.

[5] Jacob Aho, Andrew Buckspan, Jason Laks, Paul Fleming, Yunho Jeong, Fiona Dunne, Matthew Churchfield, Lucy Pao, and Kathryn Johnson. A tutorial of wind turbine control for supporting grid frequency through active power control. In *2012 American Control Conference (ACC)*, pages 3120–3131. IEEE, 2012.

[6] Jacob Aho, Paul Fleming, and Lucy Y Pao. Active power control of wind turbines for ancillary services: A comparison of pitch and torque control methodologies. In *2016 American Control Conference (ACC)*, pages 1407–1412. IEEE, 2016.

[7] Jacob Aho, Lucy Pao, and Paul Fleming. An active power control system for wind turbines capable of primary and secondary frequency control for supporting grid reliability. In *51st AIAA Aerospace Sciences Meeting including the New Horizons Forum and Aerospace Exposition*, page 456, 2013.

[8] Claude Amzallag, JP Gerey, JL Robert, and J Bahuaud. Standardization of the rainflow counting method for fatigue analysis. *International journal of fatigue*, 16(4):287–293, 1994.

[9] J. Annoni, A. Scholbrock, M. Churchfield, and P. Fleming. Evaluating tilt for wind plants. In *2017 American Control Conference (ACC)*, pages 717–722, 2017.

[10] Sirwan Ataee and Hassan Bevrani. Improvement of primary frequency control by inertial response coordination between wind and conventional power plants. *International Transactions on Electrical Energy Systems*, 27(8):e2340, 2017.

[11] Christopher J Bay, Jennifer Annoni, Timothy Taylor, Lucy Pao, and Kathryn Johnson. Active power control for wind farms using distributed model predictive control and nearest neighbor communication. In *2018 Annual American Control Conference (ACC)*, pages 682–687. IEEE, 2018.

[12] S Boersma, BM Doekemeijer, S Siniscalchi-Minna, and JW van Wingerden. A constrained wind farm controller providing secondary frequency regulation: An les study. *Renewable energy*, 134:639–652, 2019.

[13] Sjoerd Boersma, Bart Doekemeijer, Mehdi Vali, Johan Meyers, and Jan-Willem van Wingerden. A control-oriented dynamic wind farm model: Wfsim. *Wind Energy Science*, 3(1):75–95, 2018.

[14] Sjoerd Boersma, BM Doekemeijer, Pieter MO Gebraad, Paul A Fleming, Jennifer Annoni, Andrew K Scholbrock, JA Frederik, and Jan-Willem van Wingerden. A tutorial on control-oriented modeling and control of wind farms. In *2017 American Control Conference (ACC)*, pages 1–18. IEEE, 2017.

[15] M Churchfield and S Lee. Nwtc information portal (sowfa). *National Renewable Energy Laboratory*, 2014.

[16] Nicolai Cosack. Fatigue load monitoring with standard wind turbine signals. 2010.

[17] A. De Paola, D. Angeli, and G. Strbac. Scheduling of wind farms for optimal frequency response and energy recovery. *IEEE Transactions on Control Systems Technology*, 24(5):1764–1778, 2016.

[18] Simon De Rijcke, Johan Driesen, and Johan Meyers. Power smoothing in large wind farms using optimal control of rotating kinetic energy reserves. *Wind Energy*, 18(10):1777–1791, 2015.

[19] Erik Ela, V Gevorgian, P Fleming, YC Zhang, M Singh, E Muljadi, A Scholbrook, J Aho, A Buckspan, L Pao, et al. Active power controls from wind power: Bridging the gaps. Technical report, National Renewable Energy Lab.(NREL), Golden, CO (United States), 2014.

[20] Rihem Farkh, Kaouther Laabidi, and Mekki Ksouri. Pi control for second order delay system with tuning parameter optimization. 2009.

[21] Paul Fleming, Jake Aho, Pieter Gebraad, Lucy Pao, and Yingchen Zhang. Computational fluid dynamics simulation study of active power control in wind plants. In *2016 American Control Conference (ACC)*, pages 1413–1420. IEEE, 2016.

[22] Pieter MO Gebraad, FW Teeuwisse, Jan-Willem van Wingerden, Paul A Fleming, Shalom D Ruben, Jason R Marden, and Lucy Y Pao. A data-driven model for wind plant power optimization by yaw control. In *2014 American Control Conference*, pages 3128–3134. IEEE, 2014.

[23] Pieter MO Gebraad, FW Teeuwisse, JW Van Wingerden, Paul A Fleming, SD Ruben, JR Marden, and LY Pao. Wind plant power optimization through yaw control using a parametric model for wake effects—a cfd simulation study. *Wind Energy*, 19(1):95–114, 2016.

[24] Niranjan S Ghaisas, Aditya S Ghate, and Sanjiva K Lele. Effect of tip spacing, thrust coefficient and turbine spacing in multi-rotor wind turbines and farms. *Wind Energy Science*, 5(1):51–72, 2020.

[25] Jay P Goit and Johan Meyers. Optimal control of energy extraction in wind-farm boundary layers. *Journal of Fluid Mechanics*, 768:5–50, 2015.

[26] Fernando A Inthamoussou, Hernán De Battista, and Ricardo J Mantz. Lpv-based active power control of wind turbines covering the complete wind speed range. *Renewable Energy*, 99:996–1007, 2016.

[27] Tom Nørgaard Jensen, Torben Knudsen, and Thomas Bak. Fatigue minimising power reference control of a de-rated wind farm. In *Journal of Physics: Conference Series*, volume 753, page 052022. IOP Publishing, 2016.

[28] Yunho Jeong, Kathryn Johnson, and Paul Fleming. Comparison and testing of power reserve control strategies for grid-connected wind turbines. *Wind Energy*, 17(3):343–358, 2014.

[29] Jason Jonkman, Sandy Butterfield, Walter Musial, and George Scott. Definition of a 5-mw reference wind turbine for offshore system development. Technical report, National Renewable Energy Lab.(NREL), Golden, CO (United States), 2009.

[30] Jason M Jonkman, Marshall L Buhl Jr, et al. Fast user's guide. *Golden, CO: National Renewable Energy Laboratory*, 365:366, 2005.

[31] Xabier Juankorena, Iker Esandi, Jesús López, and Luis Marroyo. Method to enable variable speed wind turbine primary regulation. In *2009 International Conference on Power Engineering, Energy and Electrical Drives*, pages 495–500. IEEE, 2009.

[32] Jonas Kazda, K Merz, Nicolaos Antonio Cutululis, and John Olav Tande. Mitigating turbine mechanical loads using engineering model predictive wind farm controller. In *Journal of Physics: Conference Series*, volume 1104, page 012036. IOP Publishing, 2018.

[33] Hyungyu Kim, Kwansu Kim, and Insu Paek. Model based open-loop wind farm control using active power for power increase and load reduction. *Applied Sciences*, 7(10):1068, 2017.

[34] Kwansu Kim, Hyun-Gyu Kim, Cheol-jin Kim, Insu Paek, Carlo L Bottasso, and Filippo Campagnolo. Design and validation of demanded power point tracking control algorithm of wind turbine. *International Journal of Precision Engineering and Manufacturing-Green Technology*, 5(3):387–400, 2018.

[35] Wai Hou Lio, Mahmood Mirzaei, and Gunner Chr Larsen. On wind turbine down-regulation control strategies and rotor speed set-point. In *Journal of Physics: Conference Series*, volume 1037, page 032040. IOP Publishing, 2018.

[36] Wai Hou Alan Lio. *Blade-pitch control for wind turbine load reductions.* Springer, 2018.

[37] HT Ma and BH Chowdhury. Working towards frequency regulation with wind plants: combined control approaches. *IET Renewable Power Generation*, 4(4):308–316, 2010.

[38] Daria Madjidian. Scalable minimum fatigue control of dispatchable wind farms. *Wind Energy*, 19(10):1933–1944, 2016.

[39] Juan Manuel Mauricio, Alejandro Marano, Antonio Gómez-Expósito, and José Luis Martínez Ramos. Frequency regulation contribution through variable-speed wind energy conversion systems. *IEEE Transactions on Power Systems*, 24(1):173–180, 2009.

[40] Mahmood Mirzaei, Tuhfe Göçmen, Gregor Giebel, Poul Ejnar Sørensen, and Niels K Poulsen. Turbine control strategies for wind farm power optimization. In *2015 American Control Conference (ACC)*, pages 1709–1714. IEEE, 2015.

[41] Jackson G Njiri and Dirk Söffker. State-of-the-art in wind turbine control: Trends and challenges. *Renewable and Sustainable Energy Reviews*, 60:377–393, 2016.

[42] Romeo Ortega, Fernando Mancilla-David, and Fernando Jaramillo. A globally convergent wind speed estimator for wind turbine systems. *International Journal of Adaptive Control and Signal Processing*, 27(5):413–425, 2013.

[43] Jinkyoo Park and Kincho H Law. Layout optimization for maximizing wind farm power production using sequential convex programming. *Applied energy*, 151:320–334, 2015.

[44] Vlaho Petrović, J Schottler, I Neunaber, M Hölling, and M Kühn. Wind tunnel validation of a closed loop active power control for wind farms. In *Journal of Physics: Conference Series*, volume 1037, page 032020. IOP Publishing, 2018.

[45] Karim Saadaoui, Sami Elmadssia, and Mohamed Benrejeb. Stabilizing pid controllers for a class of time delay systems. *PID Controller Design Approaches-Theory, Tuning and Application to Frontier Areas*, 2012.

[46] Carl R Shapiro, Pieter Bauweraerts, Johan Meyers, Charles Meneveau, and Dennice F Gayme. Model-based receding horizon control of wind farms for secondary frequency regulation. *Wind Energy*, 20(7):1261–1275, 2017.

[47] S. Siniscalchi-Minna, F. D. Bianchi, and C. Ocampo-Martinez. Predictive control of wind farms based on lexicographic minimizers for power reserve maximization. In *2018 Annual American Control Conference (ACC)*, pages 701–706, 2018.

[48] Sara Siniscalchi-Minna, Fernando D Bianchi, Mikel De-Prada-Gil, and Carlos Ocampo-Martinez. A wind farm control strategy for power reserve maximization. *Renewable energy*, 131:37–44, 2019.

[49] Sara Siniscalchi-Minna, Mikel De-Prada-Gil, Fernando Daniel Bianchi, Carlos Ocampo-Martínez, and Bart De Schutter. A multi-objective predictive control strategy for enhancing primary frequency support with wind farms. In *Journal of Physics: Conference Series*, volume 1037, page 032034. IOP Publishing, 2018.

[50] Mohsen Nourbakhsh Soltani, Torben Knudsen, Mikael Svenstrup, Rafael Wisniewski, Per Brath, Romeo Ortega, and Kathryn Johnson. Estimation of rotor effective wind speed: A comparison. *IEEE Transactions on Control Systems Technology*, 21(4):1155–1167, 2013.

[51] Saurabh Srivastava and VS Pandit. A pi/pid controller for time delay systems with desired closed loop time response and guaranteed gain and phase margins. *Journal of Process Control*, 37:70–77, 2016.

[52] Mehdi Vali, V Petrović, G Steinfeld, LY Pao, and M Kühn. Large-eddy simulation study of wind farm active power control with a coordinated load distribution. In *Journal of Physics: Conference Series*, volume 1037, page 032018. IOP Publishing, 2018.

[53] Mehdi Vali, Vlaho Petrović, Sjoerd Boersma, Jan-Willem van Wingerden, and Martin Kühn. Adjoint-based model predictive control of wind farms: Beyond the quasi steady-state power maximization. *IFAC-PapersOnLine*, 50(1):4510–4515, 2017.

[54] Mehdi Vali, Vlaho Petrović, Sjoerd Boersma, Jan-Willem van Wingerden, Lucy Y Pao, and Martin Kühn. Adjoint-based model predictive control for optimal energy extraction in waked wind farms. *Control Engineering Practice*, 84:48–62, 2019.

[55] Mehdi Vali, Jan-Willem van Wingerden, Sjoerd Boersma, Vlaho Petrović, and M Kühn. A predictive control framework for optimal energy extraction of wind farms. In *Journal of Physics: Conference Series*, volume 753, page 052013. IOP Publishing, 2016.

[56] Daan van der Hoek, Stoyan Kanev, and Wouter Engels. Comparison of down-regulation strategies for wind farm control and their effects on fatigue loads. In *2018 Annual American Control Conference (ACC)*, pages 3116–3121. IEEE, 2018.

[57] MT van Dijk. A study on yaw-misaligment: Combined optimization of wind farm power production and structural loading. 2016.

[58] Jan-Willem van Wingerden, Lucy Pao, Jacob Aho, and Paul Fleming. Active power control of waked wind farms. *IFAC-PapersOnLine*, 50(1):4484–4491, 2017.

[59] Shu Wang and Peter J Seiler. Gain scheduled active power control for wind turbines. In *32nd ASME Wind Energy Symposium*, page 1220, 2014.

[60] H. Zhao, Q. Wu, Q. Guo, H. Sun, and Y. Xue. Distributed model predictive control of a wind farm for optimal active power controlpart ii: Implementation with clustering-based piece-wise affine wind turbine model. *IEEE Transactions on Sustainable Energy*, 6(3):840–849, 2015.

Glossary

List of Acronyms

WWEA	World Wind Energy Association
APC	Active Power Control
PFC	Primary Frequency Control
AGC	Automatic Generation Control
TSO	Transmission System Operator
CFD	Computational Fluid Dynamics
SWF	SimWindFarm
MPC	Model Predictive Control
PI	Proportional Integral
HAWT	Horizontal Axis Wind Turbine
TSR	Tip Speed Ratio
NREL	National Renewable Energy Laboratory
SOWFA	Simulator fOr Wind Farm Applications
FAST	Fatigue, Aerodynamics, Structures, and Turbulence
DEL	Damage Equivalent Loads